

THE STABILITY AND FATES OF HIERARCHICAL TWO-PLANET SYSTEMS

CRISTOBAL PETROVICH¹

Draft version November 5, 2018

ABSTRACT

We study the dynamical stability and fates of hierarchical (in semi-major axis) two-planet systems with arbitrary eccentricities and mutual inclinations. We run a large number of long-term numerical integrations and use the Support Vector Machine algorithm to search for an empirical boundary that best separates stable systems from systems experiencing either ejections or collisions with the star. We propose the following new criterion for dynamical stability: $a_{\text{out}}(1 - e_{\text{out}})/[a_{\text{in}}(1 + e_{\text{in}})] > 2.4 [\max(\mu_{\text{in}}, \mu_{\text{out}})]^{1/3} (a_{\text{out}}/a_{\text{in}})^{1/2} + 1.15$, which should be applicable to planet-star mass ratios $\mu_{\text{in}}, \mu_{\text{out}} = 10^{-4} - 10^{-2}$, integration times up to 10^8 orbits of the inner planet, and mutual inclinations $\lesssim 40^\circ$. Systems that do not satisfy this condition by a margin of $\gtrsim 0.5$ are expected to be unstable, mostly leading to planet ejections if $\mu_{\text{in}} > \mu_{\text{out}}$, while slightly favoring collisions with the star for $\mu_{\text{in}} < \mu_{\text{out}}$. We use our numerical integrations to test other stability criteria that have been proposed in the literature and show that our stability criterion performs significantly better for the range of system parameters that we have explored.

Subject headings: planetary systems – planets and satellites: dynamical evolution and stability

1. INTRODUCTION

More than ~ 50 exoplanet systems discovered by radial velocity (RV) surveys are known to harbor at least two planets, and many of them are in eccentric and well-separated orbits. The search for and characterization of these planets in either RV or transit surveys is generally a time-consuming task, and having an easy-to-use and accurate dynamical stability criterion is important to constrain either the existence of extra planets in the systems or the orbital configurations of already confirmed planets.

Another motivation for searching for a stability criterion comes from theoretical studies in which planets can have a variety of fates depending on the dynamical stability of a planetary system. For example, instability can lead to the formation of free-floating planets through planet ejections (e.g., Sumi et al. 2011; Veras & Raymond 2012) and planets reaching very nearly parabolic orbits can collide with or be tidally disrupted by the host star, becoming a possible source of stellar metal pollution (e.g., Sandquist et al. 2002; Zuckerman et al. 2003; Veras et al. 2013). Similarly, long-term stable and well-spaced planetary systems can evolve secularly (with no orbital energy exchange) to form close-in planets by high-eccentricity migration (e.g., Naoz et al. 2011; Wu & Lithwick 2011; Teyssandier et al. 2013; Petrovich 2015). A simple criterion to decide the fate of a planetary system based on its observed orbital configuration can help to constrain the most likely evolutionary path of different exoplanet systems without using expensive long-term N -body experiments.

There is no analytic stability criteria for arbitrary eccentricities and/or inclinations (see Georgakarakos 2008 for a review), while the currently available (semi-) empirical criteria (e.g., Harrington 1972; Eggleton & Kiseleva

1995; Mardling & Aarseth 2001) have generally not been tested in the planetary regime (in which one body contains almost all the mass of the system) or for the long timescales (up to $\sim 10^6 - 10^8$ orbits) during which two-planet systems can still become unstable (Veras & Mustill 2013; Petrovich et al. 2014).

In this study, we search for empirical criteria to decide whether a hierarchical two-planet system is likely to remain stable for long timescales or lead to either ejections or collisions with the host star. We extend previous numerical work (see §2.2) by considering a wider range of planetary systems, with planets in eccentric and/or mutually inclined orbits, and much longer evolution timescales. We also use, for the first time, the Support Vector Algorithm in the context of dynamical stability analysis, and fully detail our implementation.

2. PREVIOUS WORK ON THE STABILITY OF TWO-PLANET SYSTEMS

In this section, we briefly summarize the previous work on the stability of two-planet systems. We will use some of the stability criteria that have been proposed in the literature as benchmarks to compare to our results in §5.1.

2.1. Stability of close two-planet systems with low eccentricities

If the orbits of two planets are guaranteed to never cross, precluding collisions between planets or strong gravitational interactions, then they are said to be *Hill stable*. It has been shown that the conservation of angular momentum and energy can constrain Hill stable trajectories (Marchal & Bozis 1982; Milani & Nobili 1983).

For low eccentricities ($e \lesssim 0.1$), the Hill stability criterion can be written as (e.g., Gladman 1993)

$$\frac{a_{\text{out}}}{a_{\text{in}}} > 2.4 (\mu_{\text{in}} + \mu_{\text{out}})^{1/3} + 1, \quad (1)$$

where a_{out} (a_{in}) and μ_{in} (μ_{out}) are the semi-major axis

¹ Department of Astrophysical Sciences, Princeton University, Ivy Lane, Princeton, NJ 08544, USA; cpetrovi@princeton.edu

and planet-to-star mass ratio of the inner (outer) planets, respectively. For reference, Equation (1) implies that two Jupiter-like planets orbiting a Sun-like star are Hill stable for $a_{\text{out}} \gtrsim 1.30a_{\text{in}}$. Note that the Hill stability criterion does not discriminate mean-motion resonances.

The Hill criterion gives no information about the long-term behavior of the system, and repeated interactions between planets in Hill stable orbits can still lead to either ejections and/or collisions with the star. The orbits that are protected against either ejections or collisions with the star are referred to as *Lagrange stable*. Also, the systems that fail the Hill criterion can still avoid having close approaches and be long-term stable (see discussion §5.1).

While there is no analytic criterion for Lagrange stability, numerical studies show that the Lagrange stability boundary lies close to the Hill stability boundary (Barnes & Greenberg 2006, 2007; Deck et al. 2012). Based on the first-order mean-motion resonance overlap criterion (Wisdom 1980; Duncan et al. 1989), Deck et al. (2013) studied the conditions that can yield chaotic behavior in a two-planet system. These authors give the following criterion for the onset of chaos (which implies instability in their experiments) for two-planet systems in circular orbits:

$$\frac{a_{\text{out}}}{a_{\text{in}}} < 1.46 (\mu_{\text{in}} + \mu_{\text{out}})^{2/7} + 1. \quad (2)$$

For reference, from this criterion two Jupiter-like planets are Lagrange unstable for $a_{\text{out}} \lesssim 1.25a_{\text{in}}$. A numerical refinement of the chaotic zone boundary, which sets the stability condition above, is provided by Morrison & Malhotra (2015). Also, Veras & Mustill (2013) numerically studied the relation between the Hill and Lagrange stability boundaries for different eccentricities.

Based on this previous work, hierarchical (or well-spaced, say $a_{\text{out}} \gtrsim 2a_{\text{in}}$) and coplanar two-planet systems with low eccentricities are all expected to be long-term stable (e.g., Marzari 2014). Thus, the question of long-term stability in hierarchical two-planet systems should be focused on planets in eccentric orbits.

2.2. Stability of hierarchical two-planet systems with arbitrary eccentricities

There is no analytic criterion for the stability of hierarchical two-planet systems in eccentric orbits² and most previous works rely on numerical experiments and/or heuristic approaches. We summarize some of the dynamical stability criteria proposed for hierarchical two-planet systems. For consistency, we express each stability boundary in the form

$$r_{\text{ap}} \equiv \frac{a_{\text{out}}(1 - e_{\text{out}})}{a_{\text{in}}(1 + e_{\text{in}})} > Y \quad (3)$$

where e_{in} (e_{out}) is the eccentricity of the inner (outer) planet and Y is a function of the initial orbital elements

² Extensions to the first-order resonance overlap criterion to eccentric orbits require taking into account higher-order mean-motion resonances (e.g., Deck et al. 2013). A calculation for non-zero (but still low) eccentricities considering only first-order resonances in the test-particle approximation has been carried out by Mustill & Wyatt (2012).

and masses. This choice is motivated by our results in §4.1.1 where we find that the single parameter that best describes the stability boundary is r_{ap} .

(i) Eggleton & Kiseleva (1995) studied the stability of hierarchical triple systems with a wide range of masses and define a system to be n -stable if it preserves the initial ordering of the semi-major axes of the orbits and there are no escape orbits for 10^n orbits of the outer planet. The authors find an empirical condition for 2-stability using a set of N-body integrations, which in the planetary regime ($\mu_{\text{in}}, \mu_{\text{out}} \ll 1$) becomes:

$$r_{\text{ap}} > Y_{\text{crit}}^{\text{EK95}} \equiv 1 + 3.7\mu_{\text{out}}^{1/3} + \frac{2.2}{1 + \mu_{\text{out}}^{-1/3}} + 1.4\mu_{\text{in}}^{1/3} \frac{\mu_{\text{out}}^{-1/3} - 1}{1 + \mu_{\text{out}}^{-1/3}}. \quad (4)$$

The authors tested this criterion for $\mu_{\text{in}}, \mu_{\text{out}} \geq 0.01$ and the following sets of orbital elements: prograde coplanar orbits with either $e_{\text{in}} \in [0, 0.9]$ and $e_{\text{out}} = 0$ or $e_{\text{out}} \in [0, 0.9]$ and $e_{\text{in}} = 0$, and circular orbits with mutual inclinations $i_m \in [0, 180^\circ]$.

(ii) Mardling & Aarseth (2001) made an analogy between the stability against escape in the three-body problem and the stability against chaotic energy exchange in the binary-tides problem, and derived a semi-analytic stability criterion. We modify their criterion for coplanar and prograde orbits to express in the form of Equation (3) as

$$r_{\text{ap}} > Y_{\text{crit}}^{\text{MA01}} \equiv 2.8 \frac{(1 - e_{\text{out}})}{(1 + e_{\text{in}})} \left[(1 + \mu_{\text{out}}) \frac{1 + e_{\text{out}}}{(1 - e_{\text{out}})^{1/2}} \right]^{2/5} \quad (5)$$

This criterion does not include a dependence on e_{in} and μ_{in} , but the authors claim that it is valid for all eccentricities and masses of the inner body. Also, this criterion was proposed in the context of stellar clusters where, unlike our study, the mass ratios are not too different from unity.

(iii) The Hill stability criterion by Marchal & Bozis (1982) can be written in the planetary regime as (Gladman 1993):

$$r_{\text{ap}} > Y_{\text{crit}}^{\text{Hill}} \equiv \delta^2 \frac{(1 - e_{\text{out}})}{(1 + e_{\text{in}})}, \quad (6)$$

where δ satisfies the implicit equation

$$\frac{(\mu_{\text{in}} + \mu_{\text{out}}/\delta^2)}{(\mu_{\text{in}} + \mu_{\text{out}})^3} \left[\mu_{\text{in}} (1 - e_{\text{in}}^2)^{1/2} + \mu_{\text{out}} (1 - e_{\text{out}})^{1/2} \delta \right]^2 - 1 - 3^{4/3} \frac{\mu_{\text{in}}\mu_{\text{out}}}{(\mu_{\text{in}} + \mu_{\text{out}})^{4/3}} = 0. \quad (7)$$

The Hill stability condition has been extended by Veras & Armitage (2004) and Donnison (2006, 2011) to arbitrary mutual inclinations i_m . Even though the Hill stability might not determine the long-term stability of a two-planet system (see §2.1), we will use it as a benchmark (Barnes & Greenberg 2006, 2007). Kopparapu & Barnes (2010) numerically studied the relation between Hill and Lagrange stability and provided fitting expressions to determine the relation between these boundaries. Their results should be applicable

to planetary systems consisting of one terrestrial-mass planet and one much more massive planet with initial eccentricities less than 0.6. In this work, we focus on a complementary regime in which both the inner and the outer planets have masses much (at least ~ 30 times) larger than the Earth and therefore do not attempt to compare our results with those by Kopparapu & Barnes (2010).

(iv) Giuppone et al. (2013) proposed a semi-empirical stability criterion for eccentric two-planet systems based on Wisdom’s criterion of first-order mean-motion resonance overlap (Wisdom 1980). The authors argue that the initial value of the relative longitudes of pericenter $\Delta\varpi = \omega_{\text{in}} + \Omega_{\text{in}} - (\omega_{\text{out}} + \Omega_{\text{out}})$ can have a significant effect on the stability boundary, where ω_{in} (ω_{out}) and Ω_{in} (Ω_{out}) are the argument of pericenter and the longitude of the ascending node of the inner (outer) orbits, respectively. For the most conservative case with $\Delta\varpi = 180^\circ$ the stability boundary is given by

$$r_{\text{ap}} > Y_{\text{crit}}^{\text{GMC13}} \equiv 1 + 1.57 \left[\mu_{\text{in}}^{2/7} + \mu_{\text{out}}^{2/7} \left(\frac{a_{\text{out}}}{a_{\text{in}}} \right) \right]. \quad (8)$$

The authors also provide expressions for the case in which the ellipses are initially aligned ($\Delta\varpi = 0$), but an expression for arbitrary values of $\Delta\varpi$ is not provided.

3. NUMERICAL SIMULATIONS

We run N -body simulations of planetary systems consisting of a host star and two planets.

We use the publicly available Bulirsch-Stoer (BS) integration algorithm of MERCURY6.2 with accuracy parameter $\epsilon = 10^{-12}$ (Chambers 1999). We justify the choice of this algorithm because we are mostly interested in the evolution of dynamically active systems, where planets experience close encounters, and BS handles close encounters better than the other integration algorithms in MERCURY6.2. We simulate the evolution for a maximum time t_{max} given in units of the initial period of the inner planet $P_{\text{in},i} = 2\pi (Gm_s/a_{\text{in},i}^3)^{-1/2}$, where m_s is the mass of the central star and $a_{\text{in},i}$ is the initial semi-major axis of the inner planet. The orbital elements are given in astrometric coordinates and the typical conservation of energy and angular momentum are better than $\sim 10^{-4}$ and $\sim 10^{-6}$, respectively. We ignore the effects from general relativistic precession and tides in our calculations.

3.1. Initial conditions and input parameters

In Table 1, we summarize the input parameters, initial conditions, and outcomes of the different simulations, which are all described in the following subsections. Our fiducial simulation is *2pl-fiducial*.

The ratios between the mass of the planet and that of the host for the inner and outer orbits, μ_{in} and μ_{out} , respectively, are chosen from a uniform distribution in log over the range $[0.1M_J/M_\odot, 10M_J/M_\odot]$. The planets are treated as point masses, not allowing for planet-planet collisions. We note that the systems that would have planet collisions are expected to be unstable.

In all simulations we start with a semi-major axis ratio that is uniformly distributed in $a_{\text{out}}/a_{\text{in}} \in [3, 10]$. Thus, we generally exclude from our initial conditions the lowest-order mean-motion resonances $p : p+q$, with $p = 1$ and $q = \{2, 3, 4\}$ ($a_{\text{out}}/a_{\text{in}} = \{1.58, 2.08, 2.51\}$), which

can have a strong effect on the dynamics of the planetary system. Higher-order resonances have a weaker effect, as the strength of the resonant potential is proportional to e^q .

We draw the eccentricities of the inner and outer orbits from a uniform distribution in $[0, 0.9]$ and impose an upper limit to the eccentricity of the outer orbit $e_{\text{out}} < 1 - a_{\text{in}}/a_{\text{out}}$ to avoid a crossing of the initial orbits. Note that all the orbits very close to this boundary become unstable and thus do not contribute significant information to the derived form of the stability boundary.

For our fiducial simulation *2pl-fiducial* we initialize the mutual inclinations i_{m} between the inner and outer planetary orbits from a Rayleigh distribution with parameters $\sigma_i = 1^\circ$: the corresponding mean and median mutual inclinations are $1^\circ.25$ and $1^\circ.17$. In the simulations *2pl-inc-0* and *2pl-inc-20* we fix $i_{\text{m}} = 0$ and $i_{\text{m}} = 20^\circ$, while in *2pl-inc-rand* we initialize i_{m} from a uniform distribution in $[0, 80^\circ]$.

The arguments of pericenter, the longitudes of ascending node, and the mean anomalies are all drawn from a uniform distribution in $[0, 360^\circ]$.

3.2. Dynamical outcomes

We classify the different dynamical outcomes into the following categories.

1. *Two planets*: two planets remain in the system for a time t_{max} . Within this category, we distinguish the systems in which the initial semi-major axes of both planets have changed at a final time t_{max} by less than 10%: $|a_{\text{in},f} - a_{\text{in},i}|/a_{\text{in},i} < 0.1$ and $|a_{\text{out},f} - a_{\text{out},i}|/a_{\text{out},i} < 0.1$. These systems have experienced only a small orbital energy exchange. In the complementary category at least one of the planets has changed its initial semi-major by 10% or more.
2. *Ejection*: one planet is ejected from the system, which we define to happen when the planet reaches a distance from the central star $> 100a_{\text{in},i}$. Such planets would almost certainly escape the system because at this distance the planet is either in an escape orbit (i.e., eccentricity ≥ 1) or will most likely soon reach a escape orbit by energy perturbations from the inner planet.
3. *Stellar collision*: one planet collides with the star. This is the only scale-dependent outcome because it depends on our definition of the ratio between the stellar radius and the initial semi-major axis $R_\star/a_{\text{in},i}$. We use a fiducial conservative value for collisions of $R_\star/a_{\text{in},i} = 10^{-4}$, equivalent to placing the inner planet at $a_{\text{in},i} = 46.5$ AU for a solar-like star. We study the effect of larger values of $R_\star/a_{\text{in},i}$ in §4.2.

We treat the planets as point masses, not allowing for collisions between planets. However, for two Jupiter-size planets orbiting a Sun-size star the ratio $a_{\text{in},i}/R_J$ in our fiducial simulation is $\sim 10^5$, which is high enough that the rate of collisions between planets is expected to be very small compared to the rate of ejections or collisions with the star (e.g., Petrovich et al. 2014).

TABLE 1
SUMMARY OF SIMULATED SYSTEMS AND OUTCOMES

| Name | $a_{\text{out}}/a_{\text{in}}$ | $e_{\text{in}}, e_{\text{out}}$ | inc. [deg] | $\mu_{\text{in}}, \mu_{\text{out}}$ [M_J/M_\odot] | t_{max} [$P_{\text{in},i}$] | N_{sys} | 2 pl. with | | Ejection ($\frac{r}{a_{\text{in},i}} > 10^2$) | Stellar Coll. ($\frac{R_\star}{a_{\text{in},i}} = 10^{-4}$) |
|---------------------|--------------------------------|---------------------------------|---------------|--|---|------------------|--------------------------------|--------------------------------|--|--|
| | | | | | | | $ \frac{\Delta a}{a_i} < 0.1$ | $ \frac{\Delta a}{a_i} > 0.1$ | | |
| <i>2pl-fiducial</i> | U(x; 3,10) | U(x; 0,0.9) | Ray(1) | U(log x; -1,1) | 10^8 | 3567 | 2319 | 8 | 911 | 329 |
| <i>2pl-fid-4</i> | U(x; 3,10) | U(x; 0,0.9) | Ray(1) | U(log x; -1,1) | 10^4 | 3567 | 2917 | 390 | 212 | 48 |
| <i>2pl-fid-5</i> | U(x; 3,10) | U(x; 0,0.9) | Ray(1) | U(log x; -1,1) | 10^5 | 3567 | 2672 | 258 | 482 | 155 |
| <i>2pl-fid-6</i> | U(x; 3,10) | U(x; 0,0.9) | Ray(1) | U(log x; -1,1) | 10^6 | 3567 | 2480 | 80 | 747 | 260 |
| <i>2pl-fid-7</i> | U(x; 3,10) | U(x; 0,0.9) | Ray(1) | U(log x; -1,1) | 10^7 | 3567 | 2369 | 16 | 874 | 308 |
| <i>2pl-inc-0</i> | U(x; 3,10) | U(x; 0,0.9) | 1 | U(log x; -1,1) | 10^7 | 2000 | 1389 | 31 | 422 | 158 |
| <i>2pl-inc-20</i> | U(x; 3,10) | U(x; 0,0.9) | 20 | U(log x; -1,1) | 10^7 | 2000 | 1422 | 12 | 402 | 158 |
| <i>2pl-inc-rand</i> | U(x; 3,10) | U(x; 0,0.9) | U(x; 0,80) | U(log x; -1,1) | 10^7 | 5000 | 3319 | 37 | 1144 | 500 |

Note. $P_{\text{in},i}$ is the initial period of the inner planet. $U(x; x_{\text{min}}, x_{\text{max}})$ is the uniform distribution with $x_{\text{min}} < x < x_{\text{max}}$ and Ray(x) is the Rayleigh distribution with parameter x .

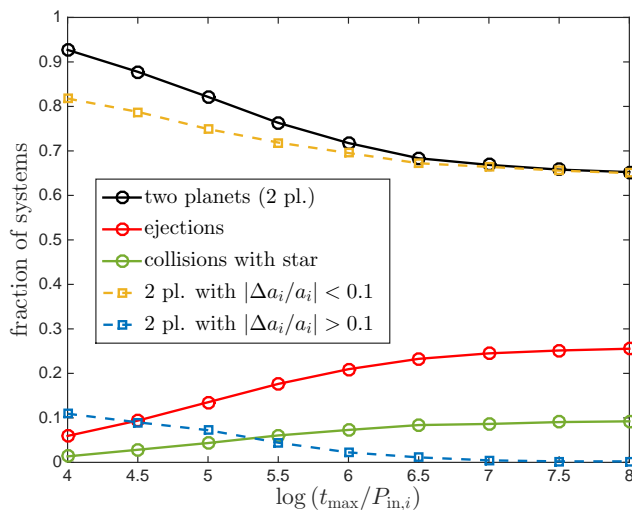


FIG. 1.— Fraction of systems with different dynamical outcomes as a function of the maximum integration time t_{max} in units of the initial orbital period of the inner planet $P_{\text{in},i}$. The dashed lines indicate the systems with two surviving planets for which at least one of the orbits has either changed its initial semi-major axis by $> 10\%$ at t_{max} (blue) or not (yellow).

3.3. Results

From Table 1, we observe that most systems ($\simeq 65\%$) in our fiducial simulation *2pl-fiducial* have two planets by the end of the simulation. Within this category over 99% are in secularly stable orbits in the sense that the planets have experienced only small orbital energy variations relative to their initial energies (the rms $\Delta a/a_i$ of the systems with $|\Delta a/a_i| < 0.1$ is $\simeq 0.3\%$, where a_i is the initial semi-major axis).

The second most common outcome ($\simeq 26\%$) is a system with one planet ejection, followed by a system with a stellar collision ($\simeq 9\%$).

The branching ratios into the different dynamical outcomes depend on various parameters, which we study next.

3.3.1. Effect of the integration timescale t_{max}

In Figure 1 and Table 1 we show the evolution of the different outcomes in our fiducial simulation as a function of the integration timescale t_{max} . In Table 1 the simulation *2pl-fid-x* corresponds to *2pl-fiducial* at $t_{\text{max}} = 10^x P_{\text{in},i}$.

From Figure 1 and Table 1, we observe that the number of systems with two planets decreases as a function of time (or t_{max}) at the expense of increasing the number of ejections and collisions with the star, as expected. This decrease is most rapid for $t_{\text{max}} < 10^6 P_{\text{in},i}$, after which time the fraction of systems with two planets (black line) shows a much slower decrease. For instance, from Table 1 we see that the number of two-planet systems decreases by $\simeq 12.6\%$ in going from 10^5 to $10^6 P_{\text{in},i}$, while it does so only by $\simeq 2.4\%$ from 10^7 to $10^8 P_{\text{in},i}$.

From Figure 1 we observe that the fraction of systems with planets having significant variations in their semi-major axes ($|\Delta a/a_i| > 0.1$, blue dashed line) decreases rapidly from $\simeq 11\%$ at $t_{\text{max}} = 10^4 P_{\text{in},i}$ to $< 0.5\%$ at $t_{\text{max}} > 10^7 P_{\text{in},i}$. Thus, almost all the systems with two planets that survive for more than $10^7 P_{\text{in},i}$ have experienced small orbital energy variations relative to their initial values and might be regarded as secularly stable systems.

In conclusion, our simulations show that there is little variation in the branching ratios of the dynamical outcomes after integrating the systems for longer than $\sim 10^7 P_{\text{in},i}$. After this time the systems with two planets are essentially all in secularly stable orbits.

3.3.2. Effect of varying $R_\star/a_{\text{in},i}$

In Figure 2, we show the fraction of systems in *2pl-fiducial* with different outcomes as a function of the ratio between the stellar radius and the initial semi-major axis of the inner planet, $R_\star/a_{\text{in},i}$.

We observe that the number of collisions with the star (green lines) increases with $R_\star/a_{\text{in},i}$, as expected. For instance, the fraction of collisions using $R_\star/a_{\text{in},i} = 10^{-4}$ ($a_{\text{in},i} \sim 50$ AU for a solar-radius star) is $\simeq 9\%$, while this ratio increases to $\simeq 15\%$ for $R_\star/a_{\text{in},i} = 10^{-2}$ ($a_{\text{in},i} \sim 0.5$ AU for a solar-radius star).

From Figure 2, we observe that the fraction of systems

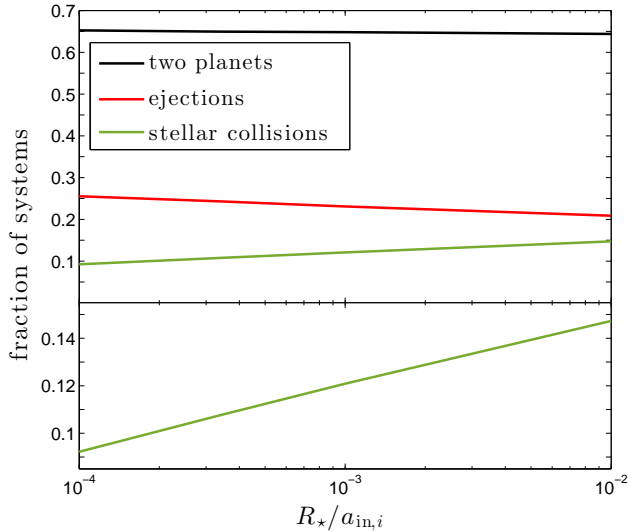


FIG. 2.— Fraction of systems in *2pl-fiducial* with different dynamical outcomes as a function of the ratio between the stellar radius and the initial semi-major axis of the inner planets $R_*/a_{in,i}$. The lower panel is a zoom-in of the fraction of systems experiencing stellar collisions.

with two planets (black line) decreases only slightly ($\sim 1\%$) by increasing $R_*/a_{in,i}$ from 10^{-4} to 10^{-2} , while the fraction of ejections decreases more significantly ($\sim 20\%$) for the same range of $R_*/a_{in,i}$.

In summary, varying $R_*/a_{in,i}$ mainly affects the ratio between ejection and collisions with the star, while the fraction of stable and unstable (ejections or collisions with the star) remains roughly constant. We shall use our conservative fiducial value of $R_*/a_{in,i} = 10^{-4}$ to determine the stability boundary in our subsequent analysis.

3.4. Effect of the mutual inclination

In Figure 3 we show the fraction of systems in *2pl-inc-rand* with different outcomes for different bins of the initial mutual inclination i_m .

The figure shows that the fraction of ejections decreases from $\simeq 0.23$ for $i_m < 10^\circ$ to $\simeq 0.16$ for $i_m \in [30^\circ, 40^\circ]$. This decrease is marginally significant and might be related to the expected reduction in the time at which the planets experience close approaches when the orbits have higher mutual inclinations. For the same range of mutual inclination $i_m < 40^\circ$ the fraction of stellar collisions does not show a clear trend. However, we observe a statistically significant decrease from $\simeq 0.09$ at $i_m \in [30^\circ, 40^\circ]$ to $\simeq 0.06$ for $i_m \in [20^\circ, 30^\circ]$.

As we start increasing the mutual inclinations from $i_m \sim 40^\circ$ there is a clear and nearly monotonic increase in the rate of both ejections and collisions with the star. This behavior might be expected since larger values of $i_m > 40^\circ$ can excite Kozai-Lidov eccentricity oscillations with large amplitudes, which can either decrease the pericenter distance to $< R_*/a_{in,i}$ producing stellar collisions, or simply increase the apocenter distance of the inner planet, promoting close encounters with the outer planet. As a consequence, the fraction of systems with two planets decreases significantly from $\simeq 0.73$ for $i_m \in [30^\circ, 40^\circ]$ to $\simeq 0.55$ for $i_m \in [70^\circ, 80^\circ]$.

In conclusion, the main effect of increasing the mutual inclination from $\sim 40^\circ$ is the enhancement of the rate of

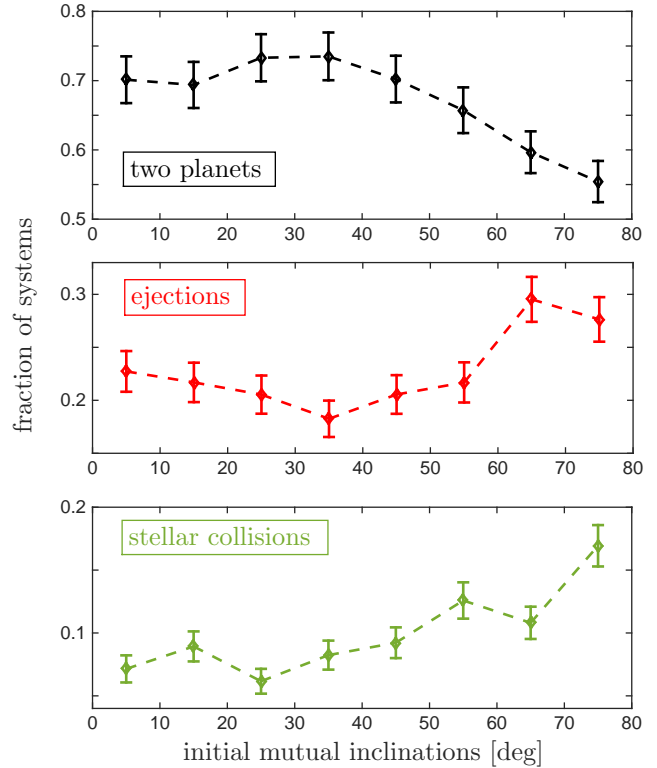


FIG. 3.— Fraction of systems in *2pl-inc-rand* at $t_{\max} = 10^7 P_{in,i}$ as a function of the initial mutual inclination of the two planets. *Upper panel:* systems with two surviving planets. *Middle panel:* systems with one planet ejection. *Lower panel:* systems with one stellar collision. The error bars indicate the Poisson counting errors for each inclination bin.

ejections and collisions with the star. As we increase the mutual inclinations from $\lesssim 10^\circ$ to $\sim 30^\circ - 40^\circ$ there is a marginally significant decrease in the rate of ejections.

4. SUPPORT VECTOR MACHINE (SVM) AND STABILITY BOUNDARY

Our main goal is to find a stability boundary that best classifies the different outcomes and is simple enough (e.g., it has a small number of parameters) to allow for easy interpretation and use. We shall assess the performance of such a classification by its degree of “completeness,” defined as the fraction of systems with true outcome X that are correctly classified as X , or the ratio between the number of true positives and the number of true positives plus the number of false negatives (e.g., Ivezić et al. 2014).

We use the Support Vector Machine (SVM) algorithm (e.g., Vapnik 1996) to separate the $i_{2pl} = 1, 2, \dots, N_{2pl}$ systems with two surviving planets from the $i_{ej} = 1, 2, \dots, N_{ej}$ systems with planet ejections and the $i_{star} = 1, 2, \dots, N_{star}$ systems with stellar collisions.

We start by defining a set of parameters α to define a classification boundary. We assume that α is a simple function of the initial orbital elements $\{a_{out}/a_{in}, e_{in}, e_{out}, \Delta\varpi, i_m\}$ and the masses $\{\mu_{in}, \mu_{out}\}$. For instance, we will define one set of parameters as $\alpha = [r_{ap}, \mu_{in}^{1/3}]$ with r_{ap} defined in Equation (3) and for each system $i = 1, 2, \dots, N_{\text{system}}$ we have a vector α_i .

We separate the classes by a hyperplane

$$f(\alpha) = \beta_0 + \beta \cdot \alpha^t, \quad (9)$$

where β_0 and β are constants obtained using SVM. We define the separating function $f(\alpha)$ such that $f(\alpha) > 0$ corresponds to systems with two planets (that is, stable systems), while $f(\alpha) < 0$ could be either ejections or collisions with the star. We classify only two classes at the time: ejections from two surviving planets in §4.1 and stellar collisions from two surviving planets in §4.2.

For each system $i = 1, 2, \dots, N_{\text{sys}}$ we calculate $f(\alpha_i)$ and we can formally define the completeness for each outcome as:

$$f_{2\text{pl}} = \frac{|f(\alpha_{i_{2\text{pl}}}) > 0|}{N_{2\text{pl}}} \quad (10)$$

$$f_{\text{ej}} = \frac{|f(\alpha_{i_{\text{ej}}}) < 0|}{N_{\text{ej}}} \quad (11)$$

$$f_{\text{star}} = \frac{|f(\alpha_{i_{\text{star}}}) < 0|}{N_{\text{star}}} \quad (12)$$

where $|\cdot|$ is the cardinality of the set of systems and $f_{2\text{pl}}, f_{\text{ej}}, f_{\text{star}} \in [0, 1]$. Thus, a function that perfectly separates ejections (stellar collisions) from two surviving planets has $f_{2\text{pl}} = f_{\text{ej}} = 1$ ($f_{2\text{pl}} = f_{\text{star}} = 1$), while a conservative stability boundary would have $f_{\text{ej}} \simeq 1$ ($f_{\text{star}} = 1$) and significantly smaller $f_{2\text{pl}}$.

We train the SVM classifier using the *fitsvm* package from Matlab 2015a with standardized variables and a linear Kernel. For our fiducial simulation, we show the performance of each separation (i.e., $f_{2\text{pl}}, f_{\text{ej}}, f_{\text{star}}$ in Table 2 and 3) using the same data as that in the training set. We have checked that the completenesses change by $\lesssim 1\%$ when a different set with ~ 1800 systems and similar initial conditions is used to test the performance of the classification.

As discussed in §3.3, the number of systems with two surviving planets in our simulations is always larger than the number of systems with either ejections or collisions with the star. Thus, the SVM algorithm would naturally tend to classify the stable systems with a higher completeness than ejections or collisions with star. Since we would like to have a boundary that separates each class with similar completeness ($f_{2\text{pl}} \sim f_{\text{ej}}$ and $f_{2\text{pl}} \sim f_{\text{star}}$), we use a cost matrix in the SVM algorithm such that the cost of classifying a system into class X if its true class is Y is $N_X/(N_X + N_Y)$. By doing so, we assign a higher penalty to misclassifying a class with a smaller number of systems.

In practice, this arbitrary procedure works well for defining boundaries with similar completenesses and it mostly changes the offset of $f(\alpha)$ by a small amount relative to the case with equal misclassification costs. Finally, we note that by artificially promoting a better classification of systems with either ejections or collisions with the stars (smaller sample) at the expense of a poorer classification of stable systems, we expect to find a more conservative stability boundary in the sense that a smaller number of unstable systems are in stable regions.

4.1. Separation of ejections and two surviving planets

We start by separating the systems with two surviving planets and from those with ejections because these classes dominate the branching ratios, and we leave the separation of stellar collisions and two planets for §4.2.

In Table 2 we show the completeness for different separating functions $f(\alpha)$ in different simulations (see Table 1). We also include a set of previously proposed stability boundaries from Equations (4), (5), (6), and (8) in §2.2. Similarly, in Figure 4 we show the distribution of the ratio between the number of systems with two surviving planets (solid black line) and ejections (red black line) and the total number of systems with either two planets or ejections for the stability boundaries above. The best criteria are those with values of f closest to unity.

4.1.1. A single parameter stability boundary:

$$f(\alpha) = \beta_0 + \beta_1\alpha$$

We start by constructing a stability boundary that only depends on one parameter, using our fiducial simulation *2pl-fiducial*. We choose the parameter to depend on only the initial orbital elements and ignore the masses because without the orbital elements the masses cannot predict the fate of a planetary system.

From Table 1, we observe that by setting $\alpha = r_{\text{ap}}$ we obtain the function $f(\alpha) = r_{\text{ap}} - 1.83$ in our fiducial simulation. For this boundary we find completenesses of $f_{2\text{pl}} \simeq 0.86$ and $f_{\text{ej}} \simeq 0.87$. Recall that by setting $\Delta\varpi = 180^\circ$, the parameter r_{ap} becomes a measure of the minimum distance d_{min} between two non-crossing coplanar orbits and $d_{\text{min}} = a_{\text{in}}(1 + e_{\text{in}})(r_{\text{ap}} - 1)$. Thus, the boundary can be rewritten as $d_{\text{min}} = 0.83 \cdot a_{\text{in}}(1 + e_{\text{in}})$; in words, the boundary classifies a system as stable if initially its orbits have a minimum distance that is at least $\simeq 83\%$ of the apocenter distance of the inner planet.

One could calculate the initial minimum distance of the two ellipses for arbitrary values $\Delta\varpi$ and construct a stability boundary using a more precise measure of the closest approaches between the planets. However, this approach has a few shortcomings:

1. the relative orientation of the orbits seems to have little effect of the performance of the stability boundary. In Table 2 we show that adding the extra parameter $\cos(\Delta\varpi)$ does not increase the values of $f_{2\text{pl}}$ and f_{ej} .
2. The resulting expression is too complicated to be of any practical use.

Based on the arguments above, we will ignore the dependence on the initial relative apsidal angles $\Delta\varpi$ in our subsequent analysis. We are aware that in a case-by-case basis, the relative orientation can certainly make a difference for the stability boundary (see the discussion in §4.1.4 and Giuppone et al. 2013).

In summary, we argue that the best single-parameter stability boundary is $r_{\text{ap}} = 1.83$ because of its simple functional form and the relatively high values of completenesses it achieves, $f_{2\text{pl}} \simeq 0.86$ and $f_{\text{ej}} \simeq 0.87$.

4.1.2. A two-parameter stability boundary:

$$f(\alpha) = \beta_0 + \beta_1\alpha_1 + \beta_2\alpha_2$$

Based on our findings above that the best single parameter to describe the stability boundary is r_{ap} , we fix $\alpha_1 \equiv r_{\text{ap}}$ and vary the functional form of α_2 to search for a two-parameter stability boundary that best separates stable systems from those with ejections in *2pl-fiducial*.

We start by including the dependence on the planet-to-star mass ratios μ_{in} and μ_{out} in $f(\alpha)$. Motivated by the

TABLE 2
SUMMARY OF FUNCTIONS $f(\alpha)$ FOUND WITH SVM AND FROM OTHER WORKS USED TO SEPARATE STABLE SYSTEMS FROM SYSTEMS WITH EJECTIONS

| Simulation | $f(\alpha)$ | $f_{2\text{pl}}$ | f_{ej} | f_{star} |
|---|---|------------------|-----------------|-------------------|
| <i>2pl-fiducial</i> | $r_{\text{ap}} - 1.83$ | 0.89 | 0.92 | 0.89 |
| <i>2pl-fiducial</i> | $r_{\text{ap}} + 0.2 \cos \Delta \varpi - 1.83$ | 0.89 | 0.92 | 0.87 |
| <i>2pl-fiducial</i> | $r_{\text{ap}} - 4\mu_{\text{in}}^{1/3} - 1.40$ | 0.91 | 0.95 | 0.80 |
| <i>2pl-fiducial</i> | $r_{\text{ap}} - 0.1\mu_{\text{out}}^{1/3} - 1.83$ | 0.89 | 0.92 | 0.83 |
| <i>2pl-fiducial</i> | $r_{\text{ap}} - 2.7(\mu_{\text{in}} + \mu_{\text{out}})^{1/3} - 1.47$ | 0.90 | 0.93 | 0.89 |
| <i>2pl-fiducial</i> | $r_{\text{ap}} - 3.8\mu_{\text{in}}^{2/7} - 1.25$ | 0.91 | 0.95 | 0.79 |
| <i>2pl-fiducial</i> | $r_{\text{ap}} - 0.82\mu_{\text{in}}^{1/3}(a_{\text{out}}/a_{\text{in}}) - 1.27$ | 0.93 | 0.95 | 0.69 |
| <i>2pl-fiducial</i> | $r_{\text{ap}} - 2.4\mu_{\text{in}}^{1/3}(a_{\text{out}}/a_{\text{in}})^{1/2} - 1.15$ | 0.94 | 0.96 | 0.75 |
| <i>2pl-fiducial</i> | $r_{\text{ap}} - 3.2\mu_{\text{in}}^{1/3}(a_{\text{out}}/a_{\text{in}})^{1/3} - 1.15$ | 0.93 | 0.96 | 0.74 |
| <i>2pl-fiducial</i> | $r_{\text{ap}} - 2.1\mu_{\text{in}}^{2/7}(a_{\text{out}}/a_{\text{in}})^{1/2} - 1.03$ | 0.94 | 0.96 | 0.75 |
| <i>2pl-fid-5</i> | $r_{\text{ap}} - 2.4\mu_{\text{in}}^{1/3}(a_{\text{out}}/a_{\text{in}})^{1/2} - 0.81$ | 0.99 | 0.96 | 0.57 |
| <i>2pl-fid-6</i> | $r_{\text{ap}} - 2.4\mu_{\text{in}}^{1/3}(a_{\text{out}}/a_{\text{in}})^{1/2} - 1.01$ | 0.97 | 0.96 | 0.65 |
| <i>2pl-fid-7</i> | $r_{\text{ap}} - 2.4\mu_{\text{in}}^{1/3}(a_{\text{out}}/a_{\text{in}})^{1/2} - 1.09$ | 0.95 | 0.96 | 0.71 |
| <i>2pl-inc-0</i> | $r_{\text{ap}} - 2.4\mu_{\text{in}}^{1/3}(a_{\text{out}}/a_{\text{in}})^{1/2} - 1.15$ | 0.93 | 0.96 | 0.68 |
| <i>2pl-inc-20</i> | $r_{\text{ap}} - 2.4\mu_{\text{in}}^{1/3}(a_{\text{out}}/a_{\text{in}})^{1/2} - 1.15$ | 0.92 | 0.95 | 0.71 |
| <i>2pl-inc-rand</i> | $r_{\text{ap}} - 2.4\mu_{\text{in}}^{1/3}(a_{\text{out}}/a_{\text{in}})^{1/2} - 1.15$ | 0.92 | 0.89 | 0.57 |
| <i>2pl-inc-rand</i> ($i_m \leq 20^\circ$) | $r_{\text{ap}} - 2.4\mu_{\text{in}}^{1/3}(a_{\text{out}}/a_{\text{in}})^{1/2} - 1.15$ | 0.92 | 0.95 | 0.71 |
| <i>2pl-inc-rand</i> ($20^\circ \leq i_m \leq 40^\circ$) | $r_{\text{ap}} - 2.4\mu_{\text{in}}^{1/3}(a_{\text{out}}/a_{\text{in}})^{1/2} - 1.15$ | 0.92 | 0.95 | 0.73 |
| <i>2pl-inc-rand</i> ($40^\circ \leq i_m \leq 60^\circ$) | $r_{\text{ap}} - 2.4\mu_{\text{in}}^{1/3}(a_{\text{out}}/a_{\text{in}})^{1/2} - 1.15$ | 0.92 | 0.90 | 0.56 |
| <i>2pl-inc-rand</i> ($60^\circ \leq i_m \leq 80^\circ$) | $r_{\text{ap}} - 2.4\mu_{\text{in}}^{1/3}(a_{\text{out}}/a_{\text{in}})^{1/2} - 1.15$ | 0.92 | 0.80 | 0.41 |
| <i>2pl-fiducial</i> | $r_{\text{ap}} - Y_{\text{crit}}^{\text{EK95}}$ | 0.92 | 0.84 | 0.87 |
| <i>2pl-fiducial</i> | $r_{\text{ap}} - Y_{\text{crit}}^{\text{MA01}}$ | 0.69 | 0.98 | 0.93 |
| <i>2pl-fiducial</i> | $r_{\text{ap}} - Y_{\text{crit}}^{\text{Hill}}$ | 0.80 | 0.77 | 0.81 |
| <i>2pl-fid-4</i> | $r_{\text{ap}} - Y_{\text{crit}}^{\text{Hill}}$ | 0.80 | 0.84 | 0.97 |
| <i>2pl-fiducial</i> | $r_{\text{ap}} - Y_{\text{crit}}^{\text{GMC13}}$ | 0.63 | 0.99 | 0.99 |

dependence of Hill's stability criterion on the planet-to-star mass ratios, we test the performance of the following parameters: $\alpha_2 = \mu_{\text{in}}^{1/3}$, $\mu_{\text{out}}^{1/3}$, and $(\mu_{\text{in}} + \mu_{\text{out}})^{1/3}$. From Table 2, we observe that the parameter that performs the best among these choices is $\alpha_2 = \mu_{\text{in}}^{1/3}$ because it reaches the highest completenesses, $f_{2\text{pl}} \simeq 0.89$ and $f_{\text{ej}} \simeq 0.92$ compared to $f_{2\text{pl}} \simeq 0.86$ and $f_{\text{ej}} \simeq 0.87$ for the one-parameter boundary. Also, we notice that incorporating the parameter $\mu_{\text{out}}^{1/3}$ provides almost no improvement in the completeness relative to the single-parameter boundary $f(\alpha) = r_{\text{ap}} - 1.83$ and SVM assigns a small multiplicative coefficient of $\beta_2 \simeq -0.1$. Finally, a stability boundary using the parameter $(\mu_{\text{in}} + \mu_{\text{out}})^{1/3}$ marginally improves the performance of the boundary relative to the single-parameter expression, but it performs worse than simply using $\mu_{\text{in}}^{1/3}$.

We have tried different power laws of the form μ_{in}^θ and found for $\theta = \{1/2, 1/3, 2/7, 1/4\}$ the highest completenesses are reached with either $1/3 \simeq 0.333$ or $2/7 \simeq 0.286$ (see Table 2). The performance is significantly (marginally) worse using $\theta = 1/2$ ($\theta = 1/4$). Based on these results our method does not distinguish between

the performance of a boundary with $\theta = 1/3$, which is expected from Hill stability (Gladman 1993) and a boundary with $\theta = 2/7$, expected from resonance overlap (Wisdom 1980). Note that Mustill & Wyatt (2012) extended the work by (Wisdom 1980) to planets with non-zero eccentricities and found a different power law with $\theta = 1/5$, which is not favored by our experiments relative to either $\theta = 1/3$ or $\theta = 2/7$.

We experimented with various simple functional forms $g(a_{\text{in}}, a_{\text{out}}, e_{\text{in}}, e_{\text{out}})$ in $\alpha_2 = \mu_{\text{in}}^{1/3} g$ and found that by setting $g = (a_{\text{in}}/a_{\text{out}})^\nu$ with $\nu > 0$ tends to increase the completeness relative to $g = 1$. In Table 1, we show the results of the stability boundaries for $\nu = \{1, 1/2, 1/3\}$ and found the best results with $\nu = 1/2$. With this index the stability boundary is

$$f = r_{\text{ap}} - 2.4\mu_{\text{in}}^{1/3}(a_{\text{out}}/a_{\text{in}})^{1/2} - 1.15, \quad (13)$$

while for a $\alpha_2 = \mu_{\text{in}}^{2/7} g$ we find:

$$f = r_{\text{ap}} - 2.1\mu_{\text{in}}^{2/7}(a_{\text{out}}/a_{\text{in}})^{1/2} - 1.03. \quad (14)$$

The boundaries in Equations (13) and (14) yield the highest completenesses in our heuristic search, $f_{2\text{pl}} =$

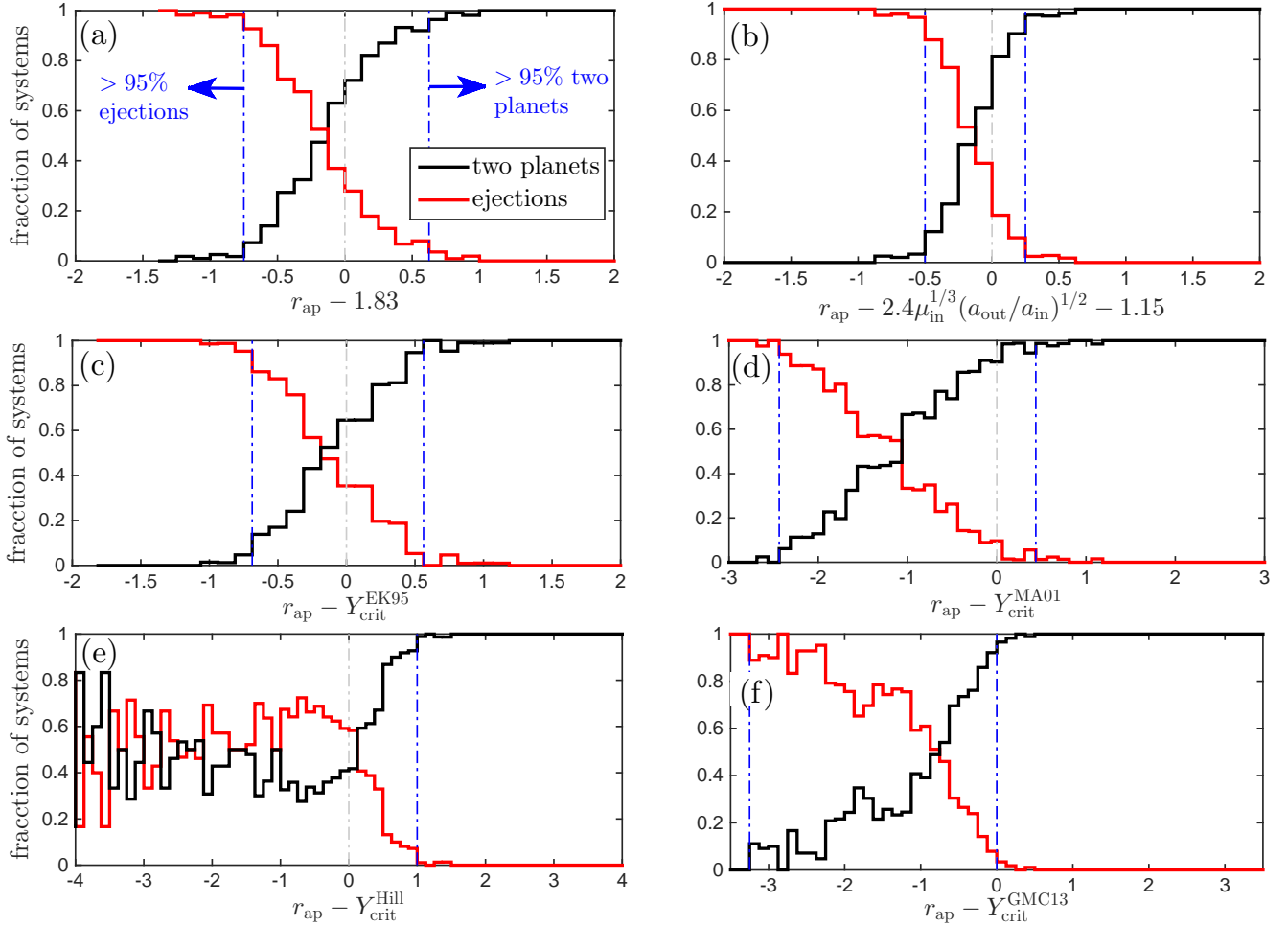


FIG. 4.— Distribution of the ratio between the number of systems with two surviving planets (solid black line) and ejections (solid red line) and the total number of systems with either two surviving planets or ejections (i.e., all systems ignoring collisions with the star) as a function of different stability boundaries. The vertical dashed-dotted blue lines indicate the regions for which $> 95\%$ of the systems to the left (right) consist of ejections (two planets). Panel (a): single-parameter boundary $f = r_{\text{ap}} - 1.83$ with $r_{\text{ap}} = a_{\text{out}}(1 - e_{\text{out}})/a_{\text{in}}(1 + e_{\text{in}})$ (see §4.1.1). Panel (b): two-parameter boundary $f = r_{\text{ap}} - 2.4\mu_{\text{in}}^{1/3}(a_{\text{out}}/a_{\text{in}})^{1/2} - 1.15$ (see §4.1.2). Panel (c): $f = r_{\text{ap}} - Y_{\text{crit}}^{\text{EK95}}$ from Eggleton & Kiseleva (1995) in Equation (4). Panel (d): $f = r_{\text{ap}} - Y_{\text{crit}}^{\text{MA01}}$ from Marling & Aarseth (2001) in Equation (5). Panel (e): $f = r_{\text{ap}} - Y_{\text{crit}}^{\text{Hill}}$ from Gladman (1993) in Equation (6). Panel (f): $f = r_{\text{ap}} - Y_{\text{crit}}^{\text{GMC13}}$ from Giuppone et al. (2013) in Equation (8). Note that the horizontal axes of panels (d), (e), and (f) are different from those in panels (a) through (c).

0.94 and $f_{\text{ej}} = 0.95$. We decided to stop here because the completenesses reached are close to unity. Also, note that we have experimented by adding an extra parameter α_3 with various functional forms and found only a marginal increase in the completenesses ($\sim 1\%$), which are at the expense of a more complicated expression of f .

In summary, we have found that the mass of the outer planet carries no information regarding the stability against planetary ejections in our simulations and we only need to know the mass of the inner planet. We have found two stability boundaries with different power-laws for the inner planet-to-star μ_{in} (Eqs. [13] and [14]), which perform the best based both on the completeness they reach when separating ejections and stable systems and on their simplicity.

4.1.3. Stability boundary and the maximum integration timescale.

We have found that a simple function that separates stable from unstable systems in *2pl-fiducial* is given

by Equation (13). Here we study the effect of the maximum integration time on this stability boundary. To do so we write the stability boundary as $r_{\text{ap}} = 2.4\mu_{\text{in}}^{1/3}(a_{\text{out}}/a_{\text{in}})^{1/2} + \gamma$ and see how γ varies with t_{max} .

In Figure 5, we show our results for γ as a function of t_{max} . We show similar results in Table 2, labeled as *2pl-fid-x* (e.g., $\gamma = 1.01$ for $t_{\text{max}} = 10^6 P_{\text{in},i}$). From Table 2, we observe that the functional form above can well separate the stable systems from ejections ($f_{2\text{pl}}, f_{\text{ej}} \gtrsim 0.95$) just by changing γ .

From Figure 5, we observe that the required value of γ increases monotonically from $\simeq 0.6$ for $\log(t_{\text{max}}/P_{\text{in},i}) = 4$ to 1.15 for $\log(t_{\text{max}}/P_{\text{in},i}) = 8$. This increase is expected because systems with larger r_{ap} (fixing the masses and semi-major axes) should become unstable later. We also observe that the coefficient γ increases more than ~ 3 times more rapidly with time from $\log(t_{\text{max}}/P_{\text{in},i}) = 4$ to $\log(t_{\text{max}}/P_{\text{in},i}) = 6$ than for $\log(t_{\text{max}}/P_{\text{in},i}) \geq 6$ (see linear fits).

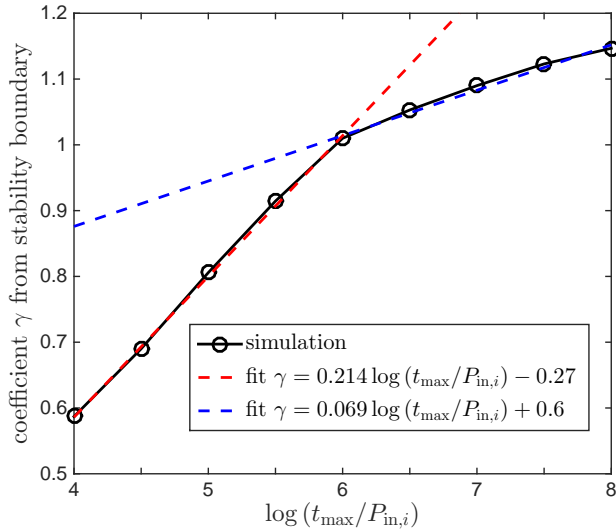


FIG. 5.— Coefficient γ from the stability boundary $r_{\text{ap}} = 2.4\mu_{\text{in}}^{1/3}(a_{\text{out}}/a_{\text{in}})^{1/2} + \gamma$ as a function of the maximum integration time t_{max} in units of the initial orbital period of the inner planet $P_{\text{in},i}$. The red and blue dashed lines indicate a linear fit for $\log(t_{\text{max}}/P_{\text{in},i}) \in [4, 6]$ and $\log(t_{\text{max}}/P_{\text{in},i}) \in [6, 8]$, respectively

From Figure 5, we fit the evolution of γ for $\log(t_{\text{max}}/P_{\text{in},i}) \geq 6$ and find that the stability boundary is given by

$$r_{\text{ap}} = 2.4\mu_{\text{in}}^{1/3} \left(\frac{a_{\text{out}}}{a_{\text{in}}} \right)^{1/2} + 0.069 \log \left(\frac{t_{\text{max}}}{P_{\text{in},i}} \right) + 0.6. \quad (15)$$

This stability boundary is valid for $t_{\text{max}}/P_{\text{in},i} = 10^6 - 10^8$ and given the slow variation of γ with time, it suggests that only a small fraction of stable systems in *2pl-fiducial* can become unstable in longer timescales.

4.1.4. Misclassified systems

Some of the stable systems ($\simeq 6\%$) are classified as ejections because they initially satisfy $r_{\text{ap}} < 2.4\mu_{\text{out}}^{1/3}(a_{\text{out}}/a_{\text{in}})^{1/2} + 1.15$. These systems tend to start with relatively aligned orbits: $\simeq 50\%$ ($\simeq 82\%$) start with $\cos \Delta\varpi > 0.8$ ($\cos \Delta\varpi > 0$). We checked that in some extreme cases, the system starts with $r_{\text{ap}} < 0$ and avoids orbit crossing by starting with $\cos \Delta\varpi \sim 1$ and engaging in a secular resonance.

Similarly, some of the systems with ejections ($\simeq 4\%$) are classified as stable because they initially satisfy $r_{\text{ap}} > 2.4\mu_{\text{out}}^{1/3}(a_{\text{out}}/a_{\text{in}})^{1/2} + 1.15$. These systems tend to start with relatively misaligned orbits: $\simeq 40\%$ ($\simeq 76\%$) start with $\cos \Delta\varpi > 0.8$ ($\cos \Delta\varpi > 0$).

By adding the extra parameter $\cos \Delta\varpi$ to our stability boundary we find $r_{\text{ap}} = 2.4\mu_{\text{out}}^{1/3}(a_{\text{out}}/a_{\text{in}})^{1/2} + 0.2 \cos \Delta\varpi + 1.1$ and the completenesses increase only marginally from $f_{2\text{pl}} \simeq 0.94$ and $f_{\text{ej}} \simeq 0.96$ to $f_{2\text{pl}} \simeq 0.94$ and $f_{\text{ej}} \simeq 0.97$.

In conclusion, some of the misclassification might be explained by the initial relative orientation of the ellipses since the orbits that start with more aligned (misaligned) pericenters tend to be more stable (unstable). These results are consistent with the claims by Giuppone et al. (2013). However, the overall effect of

$\Delta\varpi$ only marginally improves the performance from our simpler stability boundary.

TABLE 3
SUMMARY OF FUNCTIONS $f(\alpha)$ FOUND WITH SVM USED TO SEPARATE STABLE SYSTEMS FROM SYSTEMS WITH STELLAR COLLISIONS

| Simulation | $f(\alpha)$ | $f_{2\text{pl}}$ | f_{ej} | f_{star} |
|---------------------|--|------------------|-----------------|-------------------|
| <i>2pl-fiducial</i> | $r_{\text{ap}} - 1.83$ | 0.89 | 0.91 | 0.89 |
| <i>2pl-fiducial</i> | $r_{\text{ap}} + 0.47\mu_{\text{in}}^{1/3} - 1.93$ | 0.89 | 0.91 | 0.89 |
| <i>2pl-fiducial</i> | $r_{\text{ap}} - 3.4\mu_{\text{out}}^{1/3} - 1.45$ | 0.91 | 0.87 | 0.91 |
| <i>2pl-fiducial</i> | $r_{\text{ap}} - 2.7(\mu_{\text{in}} + \mu_{\text{out}})^{1/3} - 1.58$ | 0.90 | 0.93 | 0.89 |
| <i>2pl-fiducial</i> | $r_{\text{ap}} - 0.9\mu_{\text{out}}^{1/3}(a_{\text{out}}/a_{\text{in}}) - 1.18$ | 0.93 | 0.83 | 0.92 |
| <i>2pl-fiducial</i> | $r_{\text{ap}} - 2.4\mu_{\text{out}}^{1/3}(a_{\text{out}}/a_{\text{in}})^{1/2} - 1.15$ | 0.92 | 0.83 | 0.92 |

4.2. Separation of stellar collisions and two surviving planets

Following the same procedure as in §§4.1.1 and 4.1.2, we search for a stability boundary that separates systems that experience stellar collisions from systems with two surviving planets in our fiducial simulation *2pl-fiducial*.

In Table 3, we show our results for some separating functions found using SVM and their corresponding completenesses. Similarly, in Figure 6 we show the distribution of the ratio between the number of systems with two planets (solid black line) and collisions (solid red line) and the total number of systems with either two planets or collisions for different stability boundaries, including those in Equations (4)-(6), and (8) from §2.2.

From Table 3, we observe that the single-parameter boundary using r_{ap} is given by $f(\alpha) = r_{\text{ap}} - 1.83$, which is identical to that found in §4.1.1 for separating ejections from systems with two surviving planets. The completenesses using this function are $f_{2\text{pl}} = 0.89$ and $f_{\text{star}} = 0.89$.

As in §4.1.2, we include the dependence on the planet-to-star mass ratios μ_{in} and μ_{out} in $f(\alpha)$, and test the performance of the following parameters: $\alpha_2 = \mu_{\text{in}}^{1/3}$, $\mu_{\text{out}}^{1/3}$, and $(\mu_{\text{in}} + \mu_{\text{out}})^{1/3}$. From Table 3, we observe that the boundary with $\alpha_2 = \mu_{\text{in}}^{1/3}$ does not improve the performance relative to the single-parameter boundary (the completenesses are the same).

By setting $\alpha_2 = (\mu_{\text{in}} + \mu_{\text{out}})^{1/3}$ we observe that there is a slight improvement since $f_{2\text{pl}}$ increases from 0.89 in the single-parameter boundary to 0.9 and the resulting separating boundary is very similar to the one found for separating ejections from stable systems (see Table 2). Finally, by setting $\alpha_2 = \mu_{\text{out}}^{1/3}$ we find that the performance improves more significantly and the completenesses are $f_{2\text{pl}} = f_{\text{star}} = 0.91$. We tried other functional forms for the mass ratios and observed no improvements relative to $\alpha_2 = \mu_{\text{out}}^{1/3}$.

Similar to our procedure in §4.1.2, we add dependence on the semi-major axis ratio $a_{\text{out}}/a_{\text{in}}$. We find that the best separation is reached by setting $\alpha_2 = \mu_{\text{out}}^{1/3}(a_{\text{out}}/a_{\text{in}})$ with completenesses of $f_{2\text{pl}} = 0.93$ and $f_{\text{star}} = 0.92$ (see

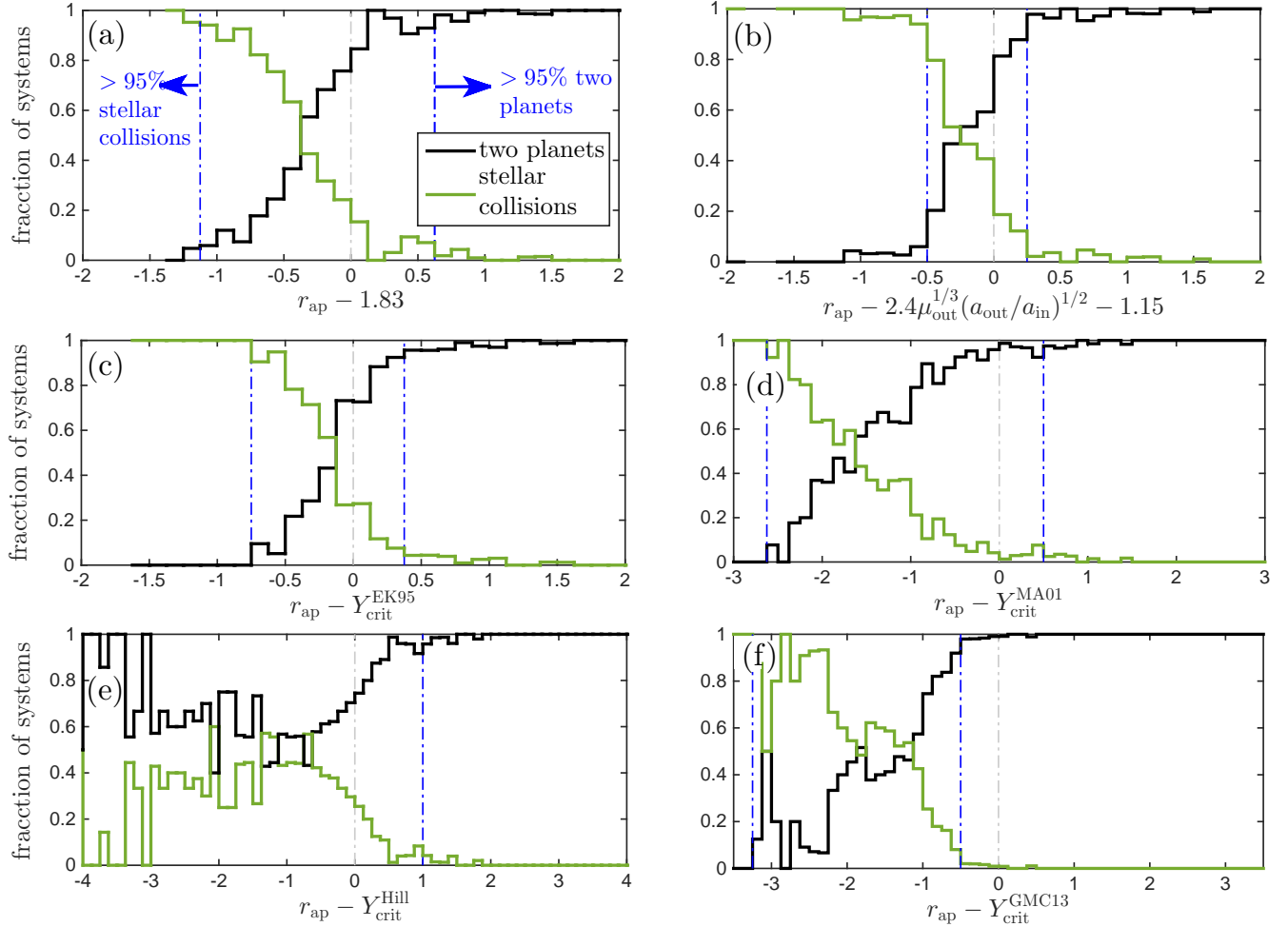


FIG. 6.— Distribution of the ratio between the number systems with two surviving planets (solid black line) and stellar collisions (solid green line) and the total number of systems with either two surviving planets or stellar collisions (i.e., all systems ignoring ejections) as a function of different stability boundaries. The vertical dashed-dotted blue lines indicate the regions for which $> 95\%$ of the systems to the left (right) consist of stellar collisions (two planets). Panel (a): single-parameter boundary $f = r_{\text{ap}} - 1.83$ with $r_{\text{ap}} = a_{\text{out}}(1 - e_{\text{out}})/a_{\text{in}}(1 + e_{\text{in}})$ (see §4.2). Panel (b): two-parameter boundary $f = r_{\text{ap}} - 2.4\mu_{\text{out}}^{1/3}(a_{\text{out}}/a_{\text{in}})^{1/2} - 1.15$ (see §4.2). Panel (c): $f = r_{\text{ap}} - Y_{\text{crit}}^{\text{EK95}}$ from Eggleton & Kiseleva (1995) in Equation (4). Panel (d): $f = r_{\text{ap}} - Y_{\text{crit}}^{\text{MA01}}$ from Mardling & Aarseth (2001) in Equation (5). Panel (e): $f = r_{\text{ap}} - Y_{\text{crit}}^{\text{Hill}}$ from Gladman (1993) in Equation (6). Panel (f): $f = r_{\text{ap}} - Y_{\text{crit}}^{\text{GM13}}$ from Giuppone et al. (2013) in Equation (8). Note that the horizontal axes of panels (d), (e), and (f) are different from those in panels (a) through (c).

Table 3). A slightly worse separation ($f_{2\text{pl}} = f_{\text{star}} = 0.92$) is reached with $\alpha_2 = \mu_{\text{out}}^{1/3}(a_{\text{out}}/a_{\text{in}})^{1/2}$, where the function reads

$$f = r_{\text{ap}} - 2.4\mu_{\text{out}}^{1/3}(a_{\text{out}}/a_{\text{in}})^{1/2} - 1.15. \quad (16)$$

This function is identical to that in Equation (13), found to separate ejections from stable systems if we change μ_{out} for μ_{in} . This surprising result suggests that the long-term stability of the system against either ejections or collisions might only depend on $\max(\mu_{\text{in}}, \mu_{\text{out}})$. Then, if an unstable system has $\mu_{\text{in}} > \mu_{\text{out}}$, the most likely outcome is an ejection, while a collision with the host star is slightly more likely if $\mu_{\text{in}} < \mu_{\text{out}}$. Motivated by these findings we favor the separating function in Equation (16) over $r_{\text{ap}} - 0.9\mu_{\text{out}}^{1/3}(a_{\text{out}}/a_{\text{in}}) - 1.18$. Finally, we have experimented with different exponents ν in $\alpha = \mu_{\text{out}}^{1/3}(a_{\text{out}}/a_{\text{in}})^\nu$ and found no improvement relative to $\nu = 1/2$.

In summary, the mass of the outer (and not the inner) planet carries most of the information about the systems that collide with the star. We found that a good stability boundary for separating collisions from stable systems is given by Equation (16), which is identical to the one found for separating ejections from stable systems when changing μ_{out} for μ_{in} .

4.3. A criterion for stability against either ejections or stellar collisions

In §4.1 and §4.2 we have found criteria for separating systems with ejections from systems with two surviving planets and systems with stellar collisions from systems with two surviving planets, respectively. In Figure 7 we show these two criteria by plotting the stability boundary against ejections in Equation (13) versus the stability boundary against collisions with the star in Equation (16) for the different outcomes in *2pl-fiducial*. We note that these criteria differ only on the whether the mass of

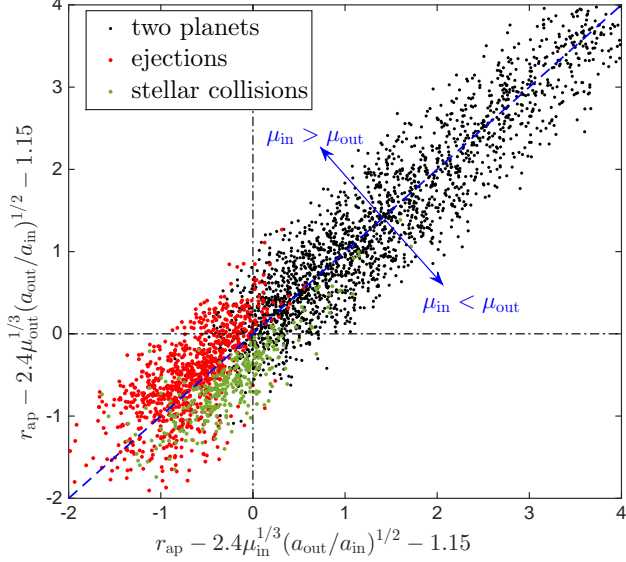


FIG. 7.— Boundary found for separating stellar collisions from stable systems from Equation (16) as a function of the boundary found for separating ejections from stable systems Equation (13) for the different outcomes in *2pl-fiducial*. The diagonal dot-dashed blue line indicate boundary in which both boundaries cross (i.e., $\mu_{\text{in}} = \mu_{\text{out}}$).

the inner and the outer is used.

We observe that most systems in regions in the positive quadrant (Equations [13] and [16] are both positive) are stable (very few red and green dots). This result suggest that we can combine Equations (13) and (16) to define a stability condition against either ejections or collisions with the star as:

$$r_{\text{ap}} > 2.4 [\max\{\mu_{\text{in}}, \mu_{\text{out}}\}]^{1/3} (a_{\text{out}}/a_{\text{in}})^{1/2} + 1.15. \quad (17)$$

This criterion yields completenesses of $f_{2\text{pl}} \simeq 0.9$ and $f_{\text{ej}+\text{star}} \simeq 0.95$. Since $f_{2\text{pl}} < f_{\text{ej}+\text{star}}$ this criterion is somewhat conservative in the sense that a smaller number of unstable systems are in stable regions relative to the number of stable systems in unstable regions.

Similarly, we observe from Figure 7 that most systems in the negative quadrant are unstable and by using the minimum instead the maximum in Equation (17) we get $f_{2\text{pl}} \simeq 0.81$ and $f_{\text{ej}+\text{star}} \simeq 0.97$. Moreover, within the unstable systems we observe that almost all of the collisions with the star ($\simeq 95\%$) are in regions where $\mu_{\text{in}} < \mu_{\text{out}}$, while most ($\simeq 72\%$) of the systems with ejections have $\mu_{\text{in}} > \mu_{\text{out}}$. Since we have an overall higher rate of ejections than stellar collisions, we find that both rates are comparable in regions where $\mu_{\text{in}} < \mu_{\text{out}}$: $\simeq 45\%$ and $\simeq 55\%$ of the unstable systems undergo ejections and collisions with the star, respectively.

In summary, we combine our previous results in Equation (17) to propose a stability boundary against either ejections or collisions with the star. Systems that are unstable and have $\mu_{\text{in}} > \mu_{\text{out}}$ will most likely undergo a planet ejection, while the systems that have $\mu_{\text{in}} < \mu_{\text{out}}$ will have a similar rate of ejections and stellar collisions, with the latter being slightly higher.

4.4. Effect of mutual inclinations on the stability boundary

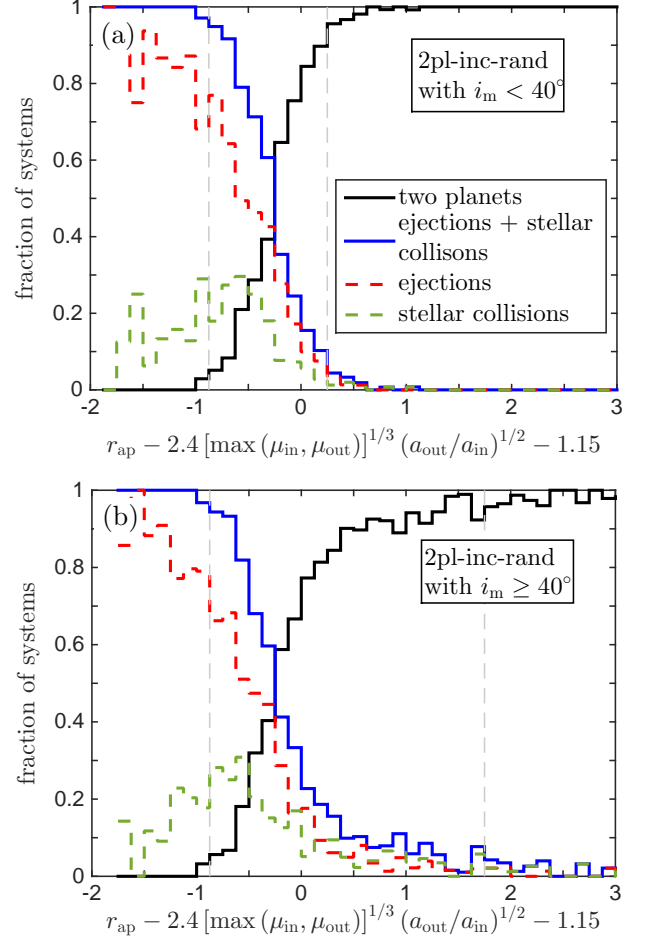


FIG. 8.— Fraction of systems with two planets (solid black line), either ejections or collisions with the star (solid blue line), ejections (dashed red line), and collisions with the star (dashed green line) in the simulation *2pl-inc-rand* as function of the stability boundary in Equation (17). *Panel a*: systems with mutual inclinations $i_m < 40^\circ$. *Panel b*: systems with mutual inclinations $i_m \geq 40^\circ$. The vertical dashed gray lines indicate the regions for which $> 95\%$ of the systems to the left (right) consist of either ejections or collisions with the star (two planets).

From Table 2 we observe that the stability boundary against ejections in Equation (13) found using *2pl-fiducial* performs relatively well in *2pl-inc-rand* ($f_{2\text{pl}} \simeq 0.92$ and $f_{2\text{pl}} \simeq 0.89$), which has a random distribution of the mutual inclination in $i_m[0, 80^\circ]$.

By taking different bins of i_m in *2pl-inc-rand* we find that the performance of the boundary in Equation (13) is the same ($f_{2\text{pl}} \simeq 0.92$ and $f_{2\text{pl}} \simeq 0.95$) for the systems starting with $i_m < 20^\circ$ and $i_m \in [20^\circ, 40^\circ]$. Similarly, the performance of this boundary in the coplanar case ($i_m = 0$) *2pl-inc-0* and in the simulation *2pl-inc-20* with $i_m = 20^\circ$ is almost the same. Thus, our stability boundary against ejections performs well for mutual inclinations $i_m \lesssim 40^\circ$.

As we increase the initial mutual inclinations in *2pl-inc-rand* we find that f_{ej} drops from $\simeq 0.95$ for $i_m < 40^\circ$ to 0.9 and 0.8 for $i_m \in [40^\circ, 60^\circ]$ and $i_m \in [60^\circ, 80^\circ]$, respectively. On the contrary, $f_{2\text{pl}}$ remains equal to $\simeq 0.92$ for all bins in mutual inclinations. As discussed in §3.4, this behavior might be expected since larger values of $i_m > 40^\circ$ can excite Kozai-Lidov eccentricity oscillations,

which can promote close encounters with the outer planet and produce ejections in regions that would be long-term stable for $i_m \lesssim 40^\circ$.

In Figure 8, we show the fraction of systems with different outcomes in our simulation *2pl-inc-rand* for $i_m < 40^\circ$ in panel (a) and $i_m \geq 40^\circ$ in panel (b) as a function of the stability criterion against either ejections or stellar collisions in Equation (17). From panel (a) we observe that there is only a small fraction of systems with either ejections or collisions with the star for $r_{\text{ap}} > 2.4 [\max\{\mu_{\text{in}}, \mu_{\text{out}}\}]^{1/3} (a_{\text{out}}/a_{\text{in}})^{1/2} + 1.15$ and $f_{\text{ej}} \simeq f_{\text{star}} \simeq f_{\text{star+ej}} \simeq 0.96$ for $i_m < 40^\circ$. From panel (b) we observe that this fraction of unstable systems in stable regions increases for $i_m < 40^\circ$ and the completenesses decrease significantly: $f_{\text{ej}} \simeq 0.87$, $f_{\text{star}} \simeq 0.67$, and $f_{\text{star+ej}} \simeq 0.8$. Since f_{star} is significantly lower than f_{ej} we conclude that the performance of our stability criterion worsens mostly at the expense of having collisions with the star in regions classified as stable. This effect is observed in Figure 8 as an increase in the tail with positive value of Equation (17) of the distribution of collisions with the star (green dashed line) in panel (b) relative to panel (a).

In summary, our stability criterion in Equation (17) performs well for mutual inclinations $i_m \lesssim 40^\circ$. For higher mutual inclinations the Kozai-Lidov mechanism produces a significant fraction of unstable systems in regions classified as stable and our criterion becomes a poor predictor for long-term stability. Our results seem consistent with a previous study by Georgakarakos (2013), which shows that the mutual inclination has very little effect on the stability boundary for $i_m \in [0, 40^\circ]$.

5. DISCUSSION

The main results of this paper are a set of new stability boundaries for separating systems that become unstable against ejections and collisions with the star from systems that retain their two planets with small orbital energy variations (Equations [13] and [16]). In particular, we propose that hierarchical two-planet systems are long-term stable if they satisfy the condition in Equation (17).

Additionally, we find that our stability boundary:

1. performs significantly better than other previously proposed criteria (see completenesses in Table 2 and 3, and Figures 4 and 6);
2. performs well for all mutual inclinations $i_m \lesssim 40^\circ$;
3. and changes slowly with the maximum integration timescale as $\propto 0.07 \log(t_{\text{max}}/P_{\text{in}})$ for $t_{\text{max}}/P_{\text{in}} = 10^6 - 10^8$, while it does so ~ 3 times more rapidly for $t_{\text{max}}/P_{\text{in}} = 10^4 - 10^6$ (see Figure 5 and Equation [15]);

The fate of the unstable systems depends mostly on the planetary masses. Most systems with $\mu_{\text{in}} > \mu_{\text{out}}$ lead to ejections, while for $\mu_{\text{in}} < \mu_{\text{out}}$ there is a slightly higher number of collisions with the star than ejections.

In what follows we discuss some of the consequences of our findings in the context of other works and the observations.

5.1. Performance of other stability criteria

In Table 2 we show the completenesses of the different stability criteria discussed in §2.2 that were reached in our fiducial simulation *2pl-fiducial*. Similarly, panels (b) to (f) in Figures 4 and 6 show the fraction of outcomes for each stability boundary. In these figures the performance is best when the outcomes have the sharpest transition from 0 to 1 (a perfect separation leads to two step-functions).

First, our simulations show that the Hill stability criterion (Equation [6] for coplanar systems) is a poor indicator of the dynamical stability of two-planet systems because it achieves relatively low completenesses ($f_{2\text{pl}} \sim f_{\text{ej}} \sim f_{\text{star}} \sim 0.8$). For comparison, even the single-parameter boundary $r_{\text{ap}} = 1.83$ performs significantly better ($f_{2\text{pl}} \sim f_{\text{ej}} \sim f_{\text{star}} \sim 0.9$). Moreover, an important fraction of the systems that are classified as Hill unstable are actually long-term stable (see the solid black lines in panel (e) of Figures 4 and 6 with $r_{\text{ap}} < Y_{\text{crit}}^{\text{Hill}}$).³

Second, we observe that both the criteria by Mardling & Aarseth (2001) and Giuppone et al. (2013) are rather conservative because they have $f_{\text{ej}}, f_{\text{star}} > 0.93$ and $f_{2\text{pl}} < 0.7$. Thus, the systems satisfying these criteria are expected to be long-term stable, but those systems that do not satisfy this condition are not necessarily expected to be unstable.

Finally, we observe that the empirical stability boundary by Eggleton & Kiseleva (1995) performs the best among the previously proposed criteria. From Table 1, we observe that $f_{2\text{pl}} \simeq 0.92$, $f_{\text{ej}} \simeq 0.84$, and $f_{\text{star}} \simeq 0.87$, which are comparable to those obtained from our one-parameter criterion $r_{\text{ap}} = 1.83$, but significantly lower than our two-parameter boundaries in Equations (13) and (16).

In summary, the stability boundary by Eggleton & Kiseleva (1995) performs the best among the previously proposed criteria, while those by Mardling & Aarseth (2001) and Giuppone et al. (2013) are too conservative. The Hill stability criterion has poor performance and provides very little useful information regarding the fate of the Hill unstable systems.

5.2. Relation to other works with more than two planets

Our results are strictly valid only for two-planet systems. However, some of our main findings can still provide useful information regarding the long-term stability in systems with more than two planets.

First, we have found that the stability boundary depends on the eccentricities only through $r_{\text{ap}} = a_{\text{out}}(1 - e_{\text{out}})/a_{\text{in}}(1 + e_{\text{in}})$, which means that the relevant quantity to describe the stability is the distance between the pericenter of the outer planet and the apocenter of the inner planet. Moreover, we show that the relative orientation of the ellipses plays only a minor role in separating a stable from unstable systems (see §4.1.4). Consistent with our results, the recent experiments by Pu & Wu (2015) show a similar dependence on the stability boundary in systems with seven planets. In their study the relevant quantity is the distance between the pericenter of the

³ Consistent with the definition of Hill stability, we have checked that in all the unstable systems with $r_{\text{ap}} > Y_{\text{crit}}^{\text{Hill}}$ it is the outer (inner) planet the one that is ejected (collides with the star). Otherwise the planets would have had orbit crossing events.

outer planet and the apocenter of the inner planet for all the adjacent planets.

Second, we find that the stability boundary changes ~ 3 times more slowly with the maximum integration time for $t_{\max}/P_{\text{in},i} < 10^6$ than in the range $t_{\max}/P_{\text{in},i} = 10^6 - 10^8$ (see Figure 5). We observe a similar behavior in the numerical experiments by Smith & Lissauer (2009), with more than two planets (see Figure 1 therein) and by Chatterjee et al. (2008) with three planets (see Figure 29 therein). There, the slope of the separation between adjacent planets required for stability as a function of $t_{\max}/P_{\text{in},i}$ decreases significantly after $\sim 10^6$ orbits of the innermost planet in the system.

Previous studies generally parameterized the spacing required for stability in units of the mutual Hill radii R_{H} as $K \equiv (a_{\text{out}} - a_{\text{in}})/R_{\text{H}} = a + b \log(t_{\max})$ (e.g., Chambers et al. 1996; Smith & Lissauer 2009), which makes it hard to make a direct quantitative comparison with our results in Equation (15). However, we can approximate our stability boundary in Equation (15) for the limit of small eccentricities (or $a_{\text{out}} - a_{\text{in}} \ll a_{\text{out}}$) and equal-mass planets ($\mu_{\text{in}} = \mu_{\text{out}}$) to write $K \propto \tilde{b}[3/(2\mu_{\text{in}})]^{1/3} \log(t_{\max})$, where \tilde{b} is the coefficient we have obtained from our simulations and the Support Vector Machine algorithm. From our fits in Figure 5, we find $\tilde{b} = 0.021$ for $t_{\max}/P_{\text{in},i} = 10^4 - 10^6$ and $\tilde{b} = 0.069$ for $t_{\max}/P_{\text{in},i} = 10^6 - 10^8$. Since our simulations have an average mass ratios $\bar{\mu}_{\text{in}} = \bar{\mu}_{\text{out}} = 10^{-3}$, we derive $K \propto 2.4 \log(t_{\max})$ for $t_{\max}/P_{\text{in},i} = 10^4 - 10^6$ and $K \propto 0.79 \log(t_{\max})$ for $t_{\max}/P_{\text{in},i} = 10^6 - 10^8$.

We notice that the slope of 0.79 that we found for $t_{\max}/P_{\text{in},i} = 10^6 - 10^8$ falls in the range of $b \sim 0.7 - 1.3$ that was found in previous studies by Smith & Lissauer (2009), Funk et al. (2010), and Pu & Wu (2015). Our results also show that it is not possible to fit the boundary with a single linear fit in $\log(t_{\max})$ since the slope b decreases as a function of time. This expectation is consistent with previous studies that predict lower values of b as the integration time increases t_{\max} : Funk et al. (2010) predict $b \sim 1.3$ for $t_{\max}/P_{\text{in},i} = 10^4 - 10^7$, Smith & Lissauer (2009) predict $b \sim 1$ for $t_{\max}/P_{\text{in},i} \lesssim 10^8$, and Pu & Wu (2015) predict $b \simeq 0.7$ for $t_{\max}/P_{\text{in},i} = 10^7 - 10^9$.

In summary, our results show that the stability boundary depends on the eccentricities only through the distance between the orbits and logarithmically on the maximum integration time, with a shallower slope for longer times. These results are qualitatively consistent with other stability studies with more than two planets.

5.3. Application to observed planetary systems

The results from our fiducial simulation *2pl-fiducial* show that (see panel (b) in Figures 4 and 6):

1. with probability > 0.95 a system is unstable if $r_{\text{ap}} < 2.4 [\max(\mu_{\text{in}}, \mu_{\text{out}})]^{1/3} + 0.6$, with ejections occurring for $\mu_{\text{in}} \geq \mu_{\text{out}}$ and either ejection or collisions with the star for $\mu_{\text{in}} < \mu_{\text{out}}$;
2. and with probability > 0.95 a system is stable against either ejections or collisions with the star if $r_{\text{ap}} > 2.4 [\max(\mu_{\text{in}}, \mu_{\text{out}})]^{1/3} (a_{\text{out}}/a_{\text{in}})^{1/2} + 1.4$.

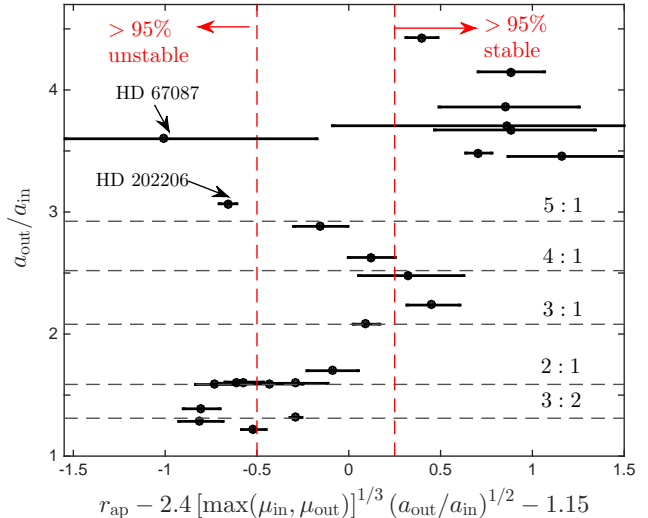


FIG. 9.— Stability boundary in Equation (17) as a function of the semi-major axis ratio $a_{\text{out}}/a_{\text{in}}$ for a sample of two-planet systems discovered by radial velocity surveys with $a_{\text{out}}/a_{\text{in}} < 5$ (from Wright et al. 2011 and HD 67087 from Harakawa et al. 2015). The error bars only consider the errors in the eccentricities and we use the minimum planet masses to calculate μ_{in} and μ_{out} . The vertical red dashed lines indicate the regions for which $> 95\%$ of the systems to the left (right) are expected to be unstable (stable) according to the stability criterion. The horizontal dashed lines indicate the position of the strongest mean-motion resonances.

In Figure 9 we show the stability boundary in Equation 17 for a sample of two-planet systems discovered by radial velocity surveys. We also display the regions for which $> 95\%$ of the systems to the left (right) are expected to be unstable (stable) according to the criterion above.

We observe that some systems are expected to be unstable according to our results. In particular, there are 3 and 4 systems around the 2 : 1 and 3 : 2 that are consistent with being left to the dashed vertical, respectively. These results might seem to contradict the validity of our stability constraints. However, our results apply to more widely-spaced systems with $a_{\text{out}}/a_{\text{in}} > 3$, where we avoid the effect from these first-order mean-motion resonances that can promote the long-term stability of the system.

A more curious case is the two-planet system HD 202206 because it has $a_{\text{out}}/a_{\text{in}} = 3.1$ and our results should apply to this range of $a_{\text{out}}/a_{\text{in}}$. As discussed by Correia et al. (2005) and Couetdic et al. (2010) such a system is indeed unstable for the best three-body fit of the RV measurements. However, there are stable coplanar solutions provided that the system is in a 5 : 1 mean-motion resonance.

Recently, Harakawa et al. (2015) discovered the planetary system HD 67087, which contains two planets with minimum masses of $\mu_{\text{in}} \sim 0.002$ and $\mu_{\text{out}} \sim 0.004$ and orbital elements $a_{\text{out}}/a_{\text{in}} \simeq 3.6_{-0.24}^{+0.24}$, $e_{\text{in}} = 0.17_{-0.07}^{+0.07}$, and $e_{\text{out}} = 0.76_{-0.24}^{+0.17}$. This system is particularly interesting because our stability criterion indicates that the systems should be unstable unless the value of e_{out} is in the lower end of its error measurement (see the error bar in Figure 9). This result suggests that the dynamical stability of this system should be further investigated, including the possibility of non-coplanar configurations

of the orbits that can lead to more stable solutions.

In conclusion, all of the observed systems (with the exception of HD 67087) that are likely to be unstable according to our criterion seem to be protected by a mean-motion resonance. The effect of mean-motion resonances does not play a significant role in our calculations because we have excluded the lowest-order mean-motion resonances $p : p + q$ with $p > 0$ and $q = \{1, 2, 3\}$ ($a_{\text{out}}/a_{\text{in}} = \{1.58, 2.08, 2.51\}$) from our calculations.

Finally, our results can be used to put constraints on the orbital elements of potential planets in systems with RV trends or poorly constrained RV measurements. In what follows, we give one worked example where we apply our stability boundary.

5.3.1. A worked example: constraints on the eccentricity of KOI-1299c.

KOI-1299 is a giant star harboring at least two giant planets (e.g., Ciceri et al. 2015; Ortiz et al. 2015; Quinn et al. 2015). The planetary system is in a hierarchical configuration with $a_{\text{out}}/a_{\text{in}} \simeq 4$ and the inner planet (KOI-1299b) is in an eccentric orbit $e_{\text{in}} \simeq 0.5$. The planet-to-mass ratios are $\mu_{\text{in}} \simeq 0.004$ and $\mu_{\text{out}} \geq 0.0018$.

Using these parameters and assuming that the planets have relatively low mutual inclinations ($i_{\text{m}} \lesssim 40^\circ$) and $\mu_{\text{in}} > \mu_{\text{out}}$, our stability constraint above implies that the system is unstable against ejections with probability $> 95\%$ if the outer planet has an eccentricity of $e_{\text{out}} \gtrsim 0.5$. Therefore, we conclude that with high probability that the eccentricity of KOI-1299c is $e_c \lesssim 0.5$. This upper limit is useful in this example because the RV measurements by Quinn et al. (2015) yield $e_c = 0.64_{-0.13}^{+0.14}$ and the error bar can be shrunk by using our stability constraint. Consistently, the authors have indeed studied the stability of this system and concluded that the system can be stable in a coplanar configuration for $\sim 6 \times 10^6$ orbits of the inner planet only if $e_c \lesssim 0.55$, which then allowed them to fit the orbital parameters to much higher accuracy, finding $e_c = 0.498_{-0.059}^{+0.029}$.

It might be surprising that the upper limit found by Quinn et al. (2015) is less constraining than the one we found with our stability boundary. However, these authors study the stability of the system surveying a much more constrained region of parameter space, confining the orbits to be almost apsidally aligned, which allows for stable orbits with higher values of e_c compared to random orientation of the orbits as we have assumed in our simulations (see §4.1.4).

We repeated the analysis above by using all the others stability boundaries shown in Figure 4 to determine an upper limit to e_c . The single-parameter boundary requires $e_c \lesssim 0.59$, while the boundary from Eggleton & Kiseleva (1995) in Equation (4) $e_c \lesssim 0.57$. All other stability boundaries that we have tested here (panels (d), (e), and (f) in Figure 4) do not provide a useful constraint as they only demand $e_c \leq 1$ for ejections not occur with probability > 0.95 .

In summary, our stability constraint places a strong constraint on the eccentricity of KOI-1299c, which is consistent with the stability analysis of Quinn et al. (2015) for this system. All other previously proposed stability boundaries, except that of Eggleton & Kiseleva (1995), do not place a useful constraint to the eccentricity of KOI-1299c.

5.4. Stellar evolution and white dwarf pollution

From Table 1, we note that the ratio between the number of stellar collisions and ejections is $\simeq 0.36$, meaning that $\simeq 27\%$ of the unstable systems reach distances $< R_\odot$ if the inner planet starts $a_{\text{in},i} = 46.5$ AU. This fraction increases up to $\simeq 41\%$ by placing the planet at $a_{\text{in},i} = 0.465$ AU (see Figure 2). Since a Jupiter-like planet orbiting a $0.6M_\odot$ white dwarf is expected to be disrupted in a highly eccentric orbit if it reaches a distance $\lesssim 3R_\odot$ (Guillochon et al. 2011), we expect that unstable hierarchical two-planet systems can often lead to tidal disruptions.

Note that most ($\simeq 95\%$) stellar collisions start with $\mu_{\text{in}} < \mu_{\text{out}}$ (see Figure 7). Also, we observe that the ratio between the number stellar collisions and the number of ejections in our fiducial simulation is $\lesssim 0.1$ for $\mu_{\text{out}}/\mu_{\text{in}} \lesssim 1.5$ and it reaches values of $\sim 1 - 3$ for $\mu_{\text{out}}/\mu_{\text{in}} \sim 2 - 6$. These results are qualitatively consistent with the increase in the ratio between the number of planets undergoing a close approach with the star and the number of ejections from $\simeq 0.03$ for equal-mass planets to $\simeq 0.12 - 0.16$ for planetary-mass ratios of $\simeq 2.3 - 3$ (randomly assigning the more massive planet as the inner one) observed by Ford & Rasio (2008). However, we observe that the overall rate of collisions with the star relative to ejections can be several times higher in our simulations for two initially eccentric planets relative to the simulations by Ford & Rasio (2008) for two planets in initially circular orbits.

Equation (15) shows that as the planetary system ages the our stability boundary becomes more stringent, allowing orbits with relatively larger separations (larger r_{ap}) to become unstable. However, the dependence is only logarithmic and the boundary moves only by $\sim 7\%$ percent per order magnitude difference in the evolution time. Thus, by extrapolating this result to timescales $> 10^8 P_{\text{in}}$ one would expect only a small effect in the stability of planetary systems.

A more pronounced effect from the aging of the planetary system is likely to come from mass loss of the host star (e.g., Debes & Sigurdsson 2002). Typical white dwarfs have masses that are a few times lower than their main-sequence progenitors and therefore the mass ratios μ_{in} and μ_{out} are expected to increase by the same factor, while keeping $a_{\text{out}}/a_{\text{in}}$ fixed (see, Veras et al. 2013; Mustill et al. 2014; Veras & Gänsicke 2015). This effect is expected to destabilize the systems close to our stability boundary in Equation (17).

In summary, unstable two-planet systems in an initially hierarchical configuration can lead to a significant number of collisions with the star relative to the number of ejections, which might contribute to the pollution of white dwarfs as a result of stellar mass loss. The number of collisions with the star (or tidal disruptions) can be higher than the number of ejections for $\mu_{\text{out}}/\mu_{\text{in}} \sim 2 - 6$.

6. CONCLUSIONS

We run a large number of long-term numerical integrations to study the fates of two-planet systems in hierarchical configurations with arbitrary eccentricities and mutual inclinations.

Using the Support Vector Machine algorithm to separate different fates of our simulated systems, we

find that initially nearly coplanar systems remain long-term stable for $a_{\text{out}}(1 - e_{\text{out}})/[a_{\text{in}}(1 + e_{\text{in}})] > 2.4 [\max(\mu_{\text{in}}, \mu_{\text{out}})]^{1/3} (a_{\text{out}}/a_{\text{in}})^{1/2} + 1.15$. Systems that do not satisfy this condition by a margin of $\gtrsim 0.5$ are expected to be unstable, mostly leading to planet ejections if $\mu_{\text{in}} > \mu_{\text{out}}$, while slightly favoring collisions with the star for $\mu_{\text{in}} < \mu_{\text{out}}$.

We show that our proposed stability boundary performs significantly better than previously proposed stability criteria (Eggleton & Kiseleva 1995, Mardling & Aarseth 2001, and Hill stability) for mutual inclinations $\lesssim 40^\circ$.

I acknowledge support from the CONICYT Bicenten-

nial Becas Chile fellowship. I am indebted to my PhD advisor Scott Tremaine, who has critically read and commented on various versions of this paper. I thank Jose Garmilla for helping me with technical issues regarding the Support Vector Machine algorithm and Dimitri Veras for helping me with technical aspects of the Mercury integrator. I am grateful to Dimitri Veras, Renu Malhotra, and Katherine Deck for enlightening discussions and comments. All simulations were carried out using computers supported by the Princeton Institute of Computational Science and Engineering. This research has made use of the Exoplanet Orbit Database and the Exoplanet Data Explorer at exoplanets.org.

REFERENCES

- Barnes, R., & Greenberg, R. 2006, *ApJ*, 647, L163
 Barnes, R., & Greenberg, R. 2007, *ApJ*, 665, L67
 Chambers, J. E. 1999, *MNRAS*, 304, 793
 Chambers, J. E., Wetherill, G. W., & Boss, A. P. 1996, *Icar*, 119, 261
 Chatterjee, S., Ford, E. B., Matsumura, S., & Rasio, F. A. 2008, *ApJ*, 686, 580
 Ciceri, S., Lillo-Box, J., Southworth, J., et al. 2015, *A&A*, 573, L5
 Correia, A. C. M., Udry, S., Mayor, M., et al. 2005, *A&A*, 440, 751
 Couetdic, J., Laskar, J., Mayor, M., & Udry, S. 2010, *A&A*, 519, A10
 Debes, J. H., & Sigurdsson, S. 2002, *ApJ*, 572, 556
 Deck, K. M., Holman, M. J., Agol, E., et al. 2012, *ApJL*, 755, L21
 Deck, K. M., Payne, M., & Holman, M. J., 2013, *ApJ*, 774, 129
 Donnison, J. R. 2006, *MNRAS*, 369, 1267
 Donnison, J. R. 2011, *MNRAS*, 415, 470
 Duncan, M., Quinn, T., & Tremaine, S. 1989, *Icar*, 82, 402
 Eggleton, P., & Kiseleva, L. 1995, *ApJ*, 455, 640
 Ford, E. B., & Rasio, F. A. 2008, *ApJ*, 686, 621
 Funk, B., Wuchterl, G., Schwarz, R., et al. S. 2010, *A&A*, 516, A82
 Georgakarakos N., 2008, *CeMDA*, 100, 151
 Georgakarakos N., 2013, *NewA*, 23, 41
 Giuppone, C. A., Morais, M. H. M., & Correia, A. C. M., 2013, *MNRAS*, 436, 3547
 Gladman, B. 1993, *Icar*, 106, 247
 Guillouchon, J., Ramirez-Ruiz, E., & Lin, D. 2011, *ApJ*, 732, 74
 Harakawa, H., Sato, B., Omiya, M. et al. 2015, *ApJ*, 806, 5
 Harrington, R. S. 1972, *CeMec*, 6, 322
 Ivezić, Ž, Connolly, A., Vanderplas, J., & Gray, A. 2014, *Statistics, Data Mining and Machine Learning in Astronomy* (Princeton, NJ: Princeton Univ. Press)
 Kopparapu, R. K., & Barnes, R. 2010, *ApJ*, 716, 1336
 Marchal, C., & Bozis, G. 1982, *CeMec*, 26, 311
 Mardling, R. A., & Aarseth, S. J. 2001, *MNRAS*, 321, 398
 Marzari, F. 2014, *MNRAS*, 442, 1110
 Milani, A., & Nobili, A. M. 1983, *CeMec*, 31, 213
 Morrison, S., & Malhotra R., 2015, *ApJ*, 799, 41
 Mustill, A. J., & Wyatt, M. C. 2012, *MNRAS*, 419, 3074
 Mustill A. J., Veras D., & Villaver E., 2014, *MNRAS*, 437, 1404
 Naoz, S., Farr, W. M., Lithwick, Y., et al. J. 2011, *Natur*, 473, 187
 Ortiz, M., Gandolfi, D., & Reffert, S. 2015, *A&A*, 573, L6
 Petrovich, C., Tremaine, S., & Rafikov, R. 2014, *ApJ*, 786, 101
 Petrovich, C. 2015, *ApJ*, 805, 75
 Pu, B., & Wu, Y. 2015, *ApJ*, 807, 44
 Quinn, S. M., White, T. R., Latham, D. W., et al 2015, *ApJ*, 805, 2
 Sandquist, E., Dokter, J., Lin, D., & Mardling, R. 2002, *ApJ*, 572, 1012
 Smith, A. W., & Lissauer, J. J. 2009, *Icar*, 201, 381
 Sumi, T., Kamiya, K., Bennett, D. P., et al. 2011, *Natur*, 473, 349
 Teyssandier, J., Naoz, S., Lizarraga, I., & Rasio, R. A. 2013, *ApJ*, 779, 166
 Vapnik, V.N 1996, *The Nature of Statistical Learning Theory* (Springer-Verlag, New York)
 Veras, D., & Armitage, P. J. 2004, *Icar*, 172, 349
 Veras, D., & Gänsicke, B. T. 2015, *MNRAS*, 447, 1049
 Veras, D., & Mustill, A. J. 2013, *MNRAS*, 434, L11
 Veras, D., Mustill, A. J., Bonsor, A., & Wyatt, M. C. 2013, *MNRAS*, 431, 1686
 Veras, D., & Raymond, S. N. 2012, *MNRAS*, 421, L117
 Wisdom, J. 1980, *AJ*, 85, 1122
 Wright J. T., Fakhouri, O., Marcy, G. W. et al. 2011, *PASP*, 123, 412
 Wu, Y., & Lithwick, Y. 2011, *ApJ*, 735,109
 Zuckerman, B., Koester, D., Reid, I. N., & Hüensch, M. 2003, *ApJ*, 596, 477